Biomedical Signal Processing and Control 84 (2023) 104979

Contents lists available at ScienceDirect

Biomedical Signal Processing and Control

journal homepage: www.elsevier.com/locate/bspc

XAI-CNVMarker: Explainable AI-based copy number variant biomarker discovery for breast cancer subtypes

Sheetal Rajpal [a], Ankit Rajpal [a,*], Manoj Agarwal [b], Virendra Kumar [c], Ajith Abraham [d], Divya Khanna [e], Naveen Kumar [a]

[a] Department of Computer Science, University of Delhi, Delhi, India
[b] Department of Computer Science, Hans Raj College, University of Delhi, Delhi, India
[c] Department of Nuclear Magnetic Resonance Imaging, All India Institute of Medical Sciences, New Delhi, India
[d] Faculty of Computing and Data Science, FLAME University, Lavale, Pune, Maharashtra, India
[e] Functional Genomics Lab, Institute of Genomics and Integrative Biology, Delhi (IGIB), India

ARTICLE INFO

Keywords:
Explainable AI
CNV
Biomarker
Deep learning
Breast cancer subtypes
Gradient

ABSTRACT

Breast cancer is a leading cause of cancer-related deaths among women. The multi-omic data has revolutionized the methodology to unravel molecular heterogeneity in breast cancer. As genetic variations captured from Copy Number Variation (CNV) data are considered the most stable amongst the multi-omic data, it leads to robust biomarkers. Thus, this paper targets the discovery of a set of CNV biomarkers for dissecting this heterogeneity. The existing algorithms yield biomarkers, too huge to be interpreted clinically. So, in this paper, we have proposed XAI-CNVMarker—an explainable AI-based post-hoc biomarker discovery framework to discover a small set of interpretable biomarkers. We exploit the power of deep learning to build *DLmodel*—a deep learning model for breast cancer classification. Subsequently, the trained model is analyzed using different explainable AI methods to arrive at a set of 44 CNV biomarkers. Using 5-fold cross-validation, we obtained a classification accuracy of 0.712 (± 0.048) at a 95% confidence interval. Gene set analysis revealed 37 subtype-specific enriched Reactome and Kegg pathways, 21 druggable genes, and 13 biomarkers linked with the prognostic outcome. Finally, we validated the efficacy of the identified biomarkers on METABRIC. Thus, the proposed framework demonstrates the role of explainable AI in discovering clinically reliable biomarkers.

1. Introduction

Breast cancer has emerged as a leading cause of mortality among women, causing 685 thousand deaths worldwide in 2020 [1]. It is a highly heterogeneous disease marked by variations at molecular and cellular levels. Traditionally, it has been labeled as in situ or invasive or classified based on histological grading, and TNM Staging. Also, Immunohistochemistry (IHC) markers (Estrogen Receptor (ER), Progesterone Receptor (PR), and human epidermal growth factor receptor 2 (Her2)) have been used to label the patients [2] with molecular subtypes as Basal, Her2, LumA, LumB, and Normal like. Whereas LumA and LumB subtypes are associated with positive levels of ER and PR receptors, LumA is characterized by Her2 negative with low Ki67, while, the LumB subtype is characterized by Her2 with high Ki67. Further, the Her2 subtype is ER/PR negative and Her2 positive. Basal-like subtype is characterized by the negative levels of all three receptors, namely, ER, PR, and Her2 [3–5]. Normal-like subtype, although somewhat similar to LumA in terms of IHC markers bears a slightly worse prognosis than LumA and corresponds to normal breast profiling.

The advent of next-generation sequencing techniques has created a wider scale of genomic, transcriptomic, and epigenomic data, in the form of copy number variation, gene expression, and methylation levels respectively. The exploration of these multi-omic data has revolutionized the way molecular mechanisms are unraveled [6–12]. Analysis of multi-omic data aids in better molecular classification of breast cancer into Basal, Her2, LumA, LumB, and Normal molecular subtypes. Towards this end, [13] proposed an intrinsic molecular classification of breast cancer, based on a set of 50 genes (called PAM50). PAM50 is considered the gold standard due to significantly better clinical and prognostic outcomes as compared to IHC-based classification [14,15] and is widely employed in practice for breast cancer classification [16–18].

As the variation in the number of copies of genes/chromosome segments is known to be associated with several cancers such as lung,

* Corresponding author.
E-mail addresses: sheetal.rajpal.09@gmail.com (S. Rajpal), arajpal@cs.du.ac.in (A. Rajpal), manoj.agarwal@hrc.du.ac.in (M. Agarwal), virendrakumar@aiims.edu (V. Kumar), ajith.abraham@ieee.org (A. Abraham), divyakh@gmail.com (D. Khanna), nkumar@cs.du.ac.in (N. Kumar).

https://doi.org/10.1016/j.bspc.2023.104979
Received 22 July 2022; Received in revised form 6 April 2023; Accepted 15 April 2023
Available online 26 April 2023

colorectal, and breast cancer [19–21], the paper investigates copy number data. Copy number data is available in two forms, namely, Copy Number Alteration (CNA) and Copy Number Variation (CNV). Whereas CNA indicates the somatic changes in the structure of chromosomes in terms of loss or gain of DNA segments that may occur during cancer progression, CNV relates to the loss or gain in terms of the number of copies of a particular gene across different patients. The variations in the copy number aid in prognosis and survival outcome [6,22]. Further, as compared to other omic data, variations in copy number are more stable [6,21]. A specific form of cancer is marked by amplification in copies of associated oncogenes and deletion of copies of the corresponding tumor suppressor genes [23,24].

Although several researchers have used CNV data in unsupervised settings with the intent to discover new clinically and prognostically relevant subtypes [25,26], a number of research leverage CNV data for discovering biomarkers for differentiating amongst the intrinsic molecular breast cancer subtypes [10,21,27] in supervised settings. Filter-based methods have been popularly used to identify gene signature [21,28,29]. Subsequently, based on the identified gene signature, standard machine learning techniques such as logistic regression, Naive Bayes, rule-based classification, support vector machine (SVM), and Random Forest (RF) have been used for the classification of breast cancer subtypes [21,28,30]. Inspired by the success of deep learning approaches in various application domains, there has been a surge in the application of deep learning techniques for the selection of an optimal set of features and for the classification of breast cancer subtypes based on the selected features [10,27,31–34]. Indeed, the deep learning approaches have also been useful for inferring the missing gene expression data [35].

As mentioned above, the discovery of CNV biomarkers representing different breast cancer subtypes is an active area of research [10, 21,27,28]. Pan et al. [21] proposed a feature selection approach for identifying informative CNV genes. They used the Monte Carlo feature selection method to identify an initial set of genes which was fed to a two-stage incremental feature selection method to arrive at the final gene signature, comprising 8715 genes. These biomarkers were used in the dagging classifier, and ensemble classifier using several base classifiers to differentiate amongst the IHC-defined breast cancer subtypes and obtained classification accuracy of 0.675 and 0.647 on METABRIC and TCGA datasets respectively. Tao et al. [28] deployed Sequential minimization optimization multiple kernel learning (SMO-MKL) for labeling IHC-defined breast cancer subtypes for patients of the TCGA dataset. For identifying features for the classification task, they used the Benjamini–Hochberg False Discovery Rate (BH-FDR) to adjust the p-values obtained by applying the Wilcoxon rank-sum test. Finally, the genes with p-values less than 0.05 were shortlisted. They reported a mean accuracy of 0.613 obtained using CNV data when performing binary classification taking two subtypes at a time, however, for the multi-class classification problem at hand, they reported approximately 0.45 accuracy. Lin et al. [10] proposed DeepMO, a deep learning network based on multi-omic data incorporating mRNA, DNA methylation, and CNV data. They used a chi-squared test for selecting the top 5000 features for each omic data. The selected feature set was provided as an input to a deep neural network comprising an encoding subnetwork and classification subnetwork. They reported mean 5-fold cross-validation accuracy of 0.525 on the TCGA dataset using CNV data. However, as mentioned above, because of the limitation of IHC-defined subtypes, another category of research incorporated widely accepted PAM50 gold standard-defined subtypes. Cristovao et al. [27] used probe-level copy number data from the TCGA repository to study heterogeneity defined by PAM50 breast cancer subtypes. Each sample comprised a vector of 1.3 million values. Pearson correlation coefficient was used to merge similar nearby regions, assigning the average copy number count to the merged region. Thus, they were able to reduce the copy number values to 384 per patient. They experimented with several supervised and semi-supervised techniques and achieved maximum accuracy of 0.706 ± 0.037 using Logistic Regression with L1 regularization (see Fig. 1).

The conventional (above-mentioned) approaches make considerable use of several machine learning and statistical methodologies for biomarker discovery. Although these approaches succeed to varying degrees in identifying CNV biomarkers for breast cancer subtypes, the contribution of the specific biomarkers remains a mystery to the end user. To ameliorate this issue, we have proposed an explainable AI-based post-hoc biomarker discovery framework—XAI-CNVMarker which intends to discover a small set of genes that exhibit variations at copy number (genomic) level across breast cancer subtypes. To the best of our knowledge, the suggested XAI-driven deep learning architecture for biomarker discovery is a unique approach to biomarker discovery. The framework would not only help with breast cancer subtyping but it may also be used by medical practitioners to develop treatment strategies. The framework incorporates the explainable AI methods, namely, (i) Gradient*Input, (ii) Integrated Gradient, (iii) Epsilon Layerwise Relevance Propagation, and (iv) DeepLIFT to arrive at a set of potential biomarkers. We first exploit the power of deep learning to build DLmodel—a deep learning model comprising an autoencoder for dimensionality reduction and a feed-forward neural network for breast cancer classification. Next, the above-mentioned explainable AI methods are used to analyze the DLmodel trained on the TCGA breast cancer CNV dataset to mark the relevance scores of the genes. Subsequently, a set of potential genes marked relevant by all the explainable AI techniques. This ensures that the most relevant genes are coherent across different interpretation methods. Further, to ensure the stability of results, the entire experimentation framework is repeated for ten random seeds leading to different weight initialization of DLmodel. Finally, only those potential genes are shortlisted as biomarkers (44) which are in the top set across 50% of the runs. While several of these 44 biomarkers are confirmed by other studies [10,21,28], we also discovered some new biomarkers such as SNOU109, MIR4642, SRGAP2B, and C1orf192. These genes encode for small nucleolar RNAs (snoRNAs), microRNAs, and proteins which play critical roles in several biological processes. These could be further studied to understand tumor heterogeneity and exploit their potential for discovering new diagnostic and therapeutic strategies.

In summary, the contributions of the paper are as follows:

1. An explainable AI-based generic framework for the discovery of copy number biomarkers associated with a clinical condition. Being comprehensible, the biomarkers so obtained will be worthy of trust for the end user.
2. Discovery of a novel set of 44 CNV biomarkers. Using these biomarkers, we achieved a five-fold cross-validation classification accuracy of 0.712 ($\pm$ 0.048) at a 95% confidence interval, which is comparable to state-of-the-art approaches.
3. Relevance of discovered biomarkers in distinguishing different breast cancer subtypes determined using SHapley Additive exPlanations (SHAP).
4. Gene set analysis revealed:
   (a) 37 enriched Reactome and Kegg pathways, such as *GRB7* events in *ERBB2*, Signaling by *FGFR1* in disease, *MAPK1/MAPK2* signaling pathway, and *PI3K-Akt* signaling pathway, known to be closely linked with different Breast Cancer subtypes.
   (b) Presence of 21 druggable genes.
   (c) Presence of 13 genes linked with the prognostic outcome.
5. Efficacy of identified CNV biomarkers, established on an independent cohort.

The remainder of the paper is organized as follows: in the second section, we describe the datasets and the proposed framework, in the third section, we provide the experimental details, results, and a discussion of the findings. Finally, the last section concludes the paper with a summarization of the results and the scope of future work.

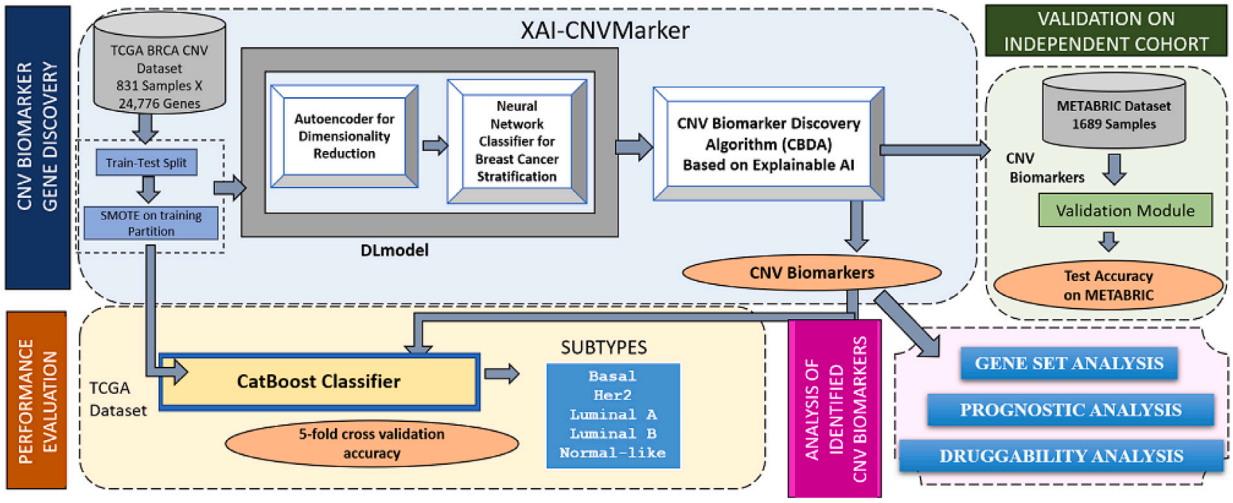

Fig. 1. Workflow of the proposed approach.

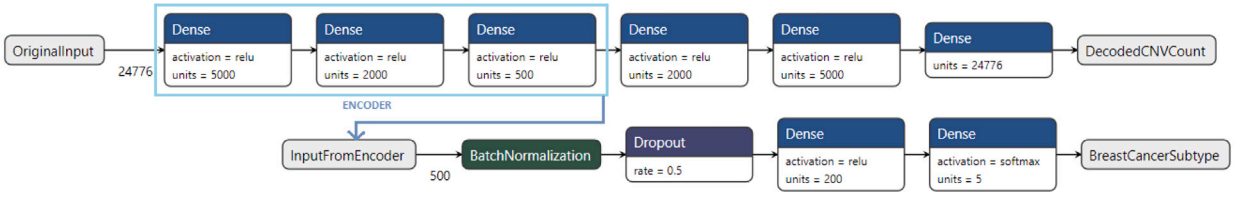

Fig. 2. *DLmodel* comprises an autoencoder module and classifier module. The encoder part of the autoencoder produces the compact representation of size 500 which is fed as input to another feed-forward classifier module.

2. Materials and methods

This section describes the datasets used for experimentation and provides a detailed description of the XAI-CNVMarker—Explainable AI-based post-hoc biomarker discovery framework. As part of this framework, we have developed a DLmodel for breast cancer classification and an Explainable AI-based CNV Biomarker Discovery Algorithm (CBDA) for identifying CNV biomarkers. Fig. 1 presents the workflow of the proposed approach. The code of the proposed framework can be accessed via https://github.com/SheetalRajpal/cnv-marker.

2.1. Dataset

The dataset used in this study is collected under TCGA (The Cancer Genome Atlas) [36] project which provides multi-omic data for several cancer types. The data set is accessed from the Xena repository maintained by the University of California. The proposed work uses gene-level CNV data. The data values include negative, zero, and positive values where the negative count indicates the number of deletions i.e., loss in the number of copies of the gene, and the positive count signifies the number of insertions (amplifications) i.e. the gain in the number of copies of genes. Although the Xena repository includes gene-level CNV data for 24,776 genes involving 1080 patients, the present study considers only 831 patients for whom PAM50 subtype labels (Basal: 135, Her2: 67, LumA: 415, LumB: 192, and Normal-like: 22) are available.

To validate the proposed framework on an independent cohort, we have used gene-level CNV data provided by METABRIC (Molecular Taxonomy of Breast Cancer International Consortium). The dataset is obtained from cBioPortal [37,38]—a multi-omic repository for Cancer Genomics. The experimentation was performed on CNV gene data for 1689 patients for whom PAM50 subtype labels were available.

2.2. DLmodel: CNV-based deep learning model for breast cancer classification

In this paper, we have proposed *DLmodel* (Fig. 2)—a deep learning model for breast cancer classification. It comprises two sub-modules. Since the high dimensional nature of the genome data poses a challenge for any classifier, in the first module, we compress the CNV data for 24 776 genes using an autoencoder. An autoencoder comprises an encoder and a decoder. The encoder network compresses a large number of input features to a small number of outputs. The outputs of the encoder network are fed to the decoder network which tries to reconstruct the original input data. The weights of the autoencoder network are optimized using the available training data by minimizing the loss of information as the inputs to the network are compressed and decompressed. In the proposed network architecture, the encoder comprises three layers. The first, second, and third layers comprise 5000, 2000, and 500 nodes, respectively. Thus, the autoencoder network maps 24,776 CNV genes to a vector of size 500. The fourth, fifth, and sixth layers of the network comprising 2000, 5000, and 24,776 nodes, respectively, form the decoder. While the hidden layers employ the ReLU activation function to handle the vanishing gradient problem, the output layer makes use of the linear activation function.

The second module of *DLmodel* is a classifier modeled as a feed-forward neural network that takes as input, the output of the encoder module of the autoencoder (a vector of size 500). The network comprises a hidden layer having 200 nodes, followed by an output layer comprising five nodes representing the five breast cancer subtypes. The hidden layer and the output layer deploy the ReLU and softmax activation functions respectively. Batch normalization has been applied to deal with the internal covariate shift problem, while Dropout (dropout rate 0.5) has been used to avoid overfitting. Fig. 2 depicts the architecture of the classifier DLmodel.

Algorithm 1: CNV Biomarker Discovery Algorithm (CBDA) for Copy Number Variation Data

Input: DLmodel: Trained Breast Cancer classification Model

X: TCGA breast cancer CNV dataset of size $N \times M$, where N denotes number of patients and M denotes number of genes.

Methods Used:

explainAIMethod($DLmodel$, X): For every patient x of dataset X, the function returns relevance score of each gene in classifying the patient using the trained network DLmodel.

elbowMethod($scoreMatrix$): For each patient in the given set, function returns top genes with maximum relevance score computed using elbow method.

topAverageGenes($scoreMatrix, n$): For each subtype in the given set, function returns top n genes with maximum average relevance score.

select($list$, $threshold$): Returns those genes from the given list, having threshold as its minimum count of occurrence.

frequentAcrossMethods($list$, $threshold$): Returns those genes from the given list, having threshold as its minimum count of occurrence.

frequentAcrossSeeds($list$, $threshold$): Returns those genes from the given list, having threshold as its minimumcount of occurrence.

def subtypeSpecificMarkers (DLmodel, X) :

1. for $subtype$ in $PAM50\_Subtypes$ do
   (a) $geneSetVector[subtype] \leftarrow \{\}$
2. for $explainAIMethod$ in $Gradient*input$, $EpsilonLRP$, $DeepLIFT$, $IntegratedGradient$, do
   (a) $scores \leftarrow explainAIMethod(DLmodel, X)$
   (b) for $subtype$ in $PAM50\_Subtypes$ do
      i. $topGenes \leftarrow elbowMethod(scores[X[subtype]])$
      ii. $threshold \leftarrow len(X[subtype])/5$
      iii. $geneSet[explainAIMethod, subtype] \leftarrow select(topGenes, threshold) \cup topAverageGenes(scores[X[subtype]], n)$
      iv. $geneSetVector[subtype] \leftarrow geneSetVector[subtype] \cup geneSet[explainAIMethod, subtype]$
3. for $subtype$ in $PAM50\_Subtypes$ do
   (a) $potentialSet[subtype] \leftarrow frequentAcrossMethods(geneSetVector[subtype], threshold)$
4. Return [potentialSet[subtype1], potentialSet[subtype2], potentialSet[subtype3], potentialSet[subtype4], potentialSet[subtype5]]

def biomarkerDiscovery( ) :

1. $ShortlistedGenes \leftarrow \{\}$
2. for $seed$ in $Different\_k\_Seeds$ do
   (a) $model \leftarrow DLmodel(seed, X)$
   (b) $ShortlistedGenes[Allsubtypes] \leftarrow ShortlistedGenes[Allsubtypes] \cup subtypeSpecificMarkers(model)$
3. for $subtype$ in $PAM50Subtypes$ do
   (a) $Biomarkers[subtype] \leftarrow frequentAcrossSeeds(ShortlistedGenes[subtype], threshold)$
4. Return $Biomarkers$

2.3. CBDA: CNV biomarker discovery algorithm: an explainable AI approach

In this section, we have proposed a CNV Biomarker Discovery Algorithm (CBDA) that uses an explainable AI modeling approach to identify CNV biomarkers for breast cancer subtype classification. Explainable AI intends to uncover the contribution of input features by analyzing the behavior of deployed computational models. Thus, it helps in building the trust of clinicians in the methodology and the discovered biomarkers. The details of the approach appear in Algorithm 1. In this work, we use four explainable AI methods, namely, Gradient*input, Integrated Gradient, Epsilon Layerwise Relevance Propagation, and DeepLIFT (description mentioned in appendix) to discover a small set of CNV biomarkers.

The execution of the CBDA algorithm begins by invoking the function *biomarkerDiscovery*. First, an empty set of $ShortlistedGenes$ is created (step 1). In step 2, it builds k (= 10) DLmodel (one for each seed) for breast cancer subtype classification using CNV data (step 2a). Each of the models is analyzed using function $subtypeSpecificMarkers$ and the genes contributing towards the model's prediction are shortlisted (step 2b). For patients of each subtype, the function $subtypeSpecificMarkers$ selects the most differentiating genes ($geneSetVector$) using four explainable AI methods. The function $subtypeSpecificMarkers$ begins with an empty vector of a set of genes $geneSetVector$, each component of which is associated with a subtype (step 1a). $geneSetVector$ is updated incrementally in step 2b(iv) by adding genes relevant to each specific subtype for all the explainable AI methods. $explainAIMethod$ method is used to compute the $scores$ (relevance) of various genes by analyzing the $DLmodel$ using the entire dataset X (step 2a). Next, given a $subtype$, we pick the $topGenes$ based on their relevance scores using $elbowMethod$ (step 2b(i)). For each subtype, we finally select a set of genes ($geneSetVector$) that are included in the set of $topGenes$ for a fraction (threshold of 20%) of patients of this subtype (steps 2b(ii) and 2b(iii)). Moreover, we also

include those genes in the $geneSetVector$ with the maximum average relevance score for the subtype in consideration.

Finally, from the subtype-specific genes ($geneSetVector$), those genes are shortlisted as potential biomarkers which are marked as relevant by all the four explainable AI methods (step 3a). These subtype-specific copy number biomarkers are returned to function $biomarkerDiscovery$ after the interpretation of every trained model initialized using different seeds (step 4). In the $biomarkerDiscovery$ function, finally, only those genes are selected as biomarkers for each of the subtypes which are identified as most contributing to the predicted class for at least 50% of the seeds (step 3a).

3. Experimental results and discussion

In this section, we present details of experiments and results. We begin with a description of data preprocessing and hyperparameter tuning. Next, we discuss the discovery of CNV biomarker genes using the proposed framework *XAI-CNVMarker* and their effectiveness in breast cancer subtype classification. Further, we evaluate the trustworthiness of the discovered biomarkers in terms of their biological relevance. In this regard, we report the results of Reactome pathways enriched, potentially druggable genes, and prognostic analysis of the identified CNV biomarkers. Finally, we report the results of validation on an independent cohort.

3.1. Experimental details

All experiments have been performed in Python 3.7 in the Google Colaboratory using a runtime environment for NVIDIA Tesla K80 GPU. For data pre-processing, model construction, and visualization, Python libraries namely, Pandas, Numpy, Imblearn, Keras, Matplotlib, Scikit-Learn, and Seaborn have been used. Methods of the DeepExplain tool and SHAP libraries have been applied for the purpose of explainability.

3.1.1. Data pre-processing

For 831 patients under study, We mapped PAM50 subtypes, namely, Basal, Her2, LumA, LumB, and Normal to numerical values of 0, 1, 2, 3, and 4. Further, each subtype was transformed into the corresponding one-hot encoding vector. For evaluating the performance of the classifier, 5-fold stratified cross-validation is used with an equal fraction of samples of each class in each fold. The classification process is repeated five times, retaining one of the folds as the test data and the combined data in the remaining folds as the training data. Further, $1/10^{th}$ of the 80% of the data used for training is used as a validation set for steering model construction. In view of the skewed distribution of samples (see Fig. 3), we applied a Synthetic Minority Oversampling Technique (SMOTE) filter [39] on the training data to avoid the risk of the trained model is biased towards the majority class.

3.1.2. Hyperparameter tuning of DLmodel

As mentioned in Section 2, hidden layers of the DLmodel employ the ReLU activation function to overcome the vanishing gradient problem. The first sub-module of DLmodel comprising autoencoder uses the mean squared loss function and Adam optimizer with a learning rate of 0.0002. We used a batch size of 80 during training. To prevent the network from overfitting, early stopping criteria (decrease in validation loss (δ) = 0.001, patience level = 100) was used. We also experimented with shallower architectures of autoencoder, however, the resulting classifiers did not work well. We observed that the model stopped learning after a few iterations. In the feed-forward classifier network of the second sub-module of DLmodel, categorical cross entropy loss function and Adam optimizer (learning rate = 0.0002) were used. We have trained the model for 1000 epochs, using a batch size of 64. Further, during training, we used checkpoints to save the weights of the network yielding the maximum validation accuracy.

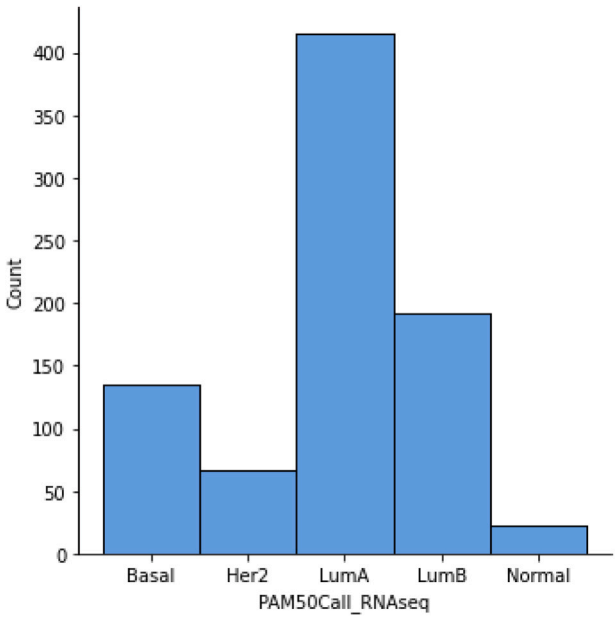

Fig. 3. Class distribution of samples.

3.1.3. Neural network classifier results based on 24,776 input genes

Two sub-networks of DLmodel are trained separately. The encoded representation of CNV data obtained from the autoencoder is passed to the second sub-network that classifies breast cancer patients into five PAM50-defined subtypes. The trained model is used for evaluating the performance on the test set using 5-fold cross-validation. Using the entire set of 24,776 genes, we obtained classification accuracy of 0.683 $\pm$ 0.05 at 95% confidence interval using 5-fold cross-validation. Thus, we conclude that the proposed framework is quite stable. However, it uses the entire set of genes.

3.2. Using explainable AI for selection of biomarkers and their classification performance

We have applied the CNV Biomarker Discovery Algorithm (CBDA) algorithm of the proposed framework *XAI-CNVMarker* described in Section 2.3 for discovering the CNV biomarkers for breast cancer subtypes. In CNV Biomarker Discovery Algorithm (CBDA), we initially experimented with several model-specific explainable AI methods, namely, Gradient, Guided Backpropagation, Smooth Gradient, Gradient*input, Integrated Gradient, Epsilon Layerwise Relevance Propagation, and DeepLIFT, to examine the trained DLmodel. The candidate gene set discovered by each of the methods was evaluated independently to assess their efficacy in distinguishing different breast cancer subtypes. We found that the methods, namely, Gradient, Guided Backpropagation, and Smooth Gradient yielded gene sets leading to lower accuracy in the range (63, 66). Moreover, the gene set identified as relevant by these methods shared very little overlap with each other or with the other methods used. In contrast, Gradient * input, Integrated Gradient, Epsilon Layerwise Relevance Propagation, and DeepLIFT, yielded gene sets leading to higher accuracy (> 67). To ensure the trustworthiness of the identified biomarkers, in CBDA, we selected only those genes in the final set of biomarkers that were marked relevant by each of the aforementioned four methods.

As discussed earlier, we analyzed the $DLmodel$ using different explainable AI methods to arrive at a set of 44 biomarkers for breast cancer classification. These biomarkers include *ANKRD11*, *ANO1*, *ATAD2*, *C1orf189*, *CASC8*, *CCND1*, *CDK12*, *CTSF*, *DDR2*, *DDX19A*, *ERBB2*, *ERLIN2*, *FADD*, *FAM91A1*, *FGF19*, *FGF4*, *FGFR1*, *GADD45A*, *GPR124*, *GRB7*, *IKZF3*, *ISG20L2*, *KRT6C*, *LCAT*, *LMOD1*, *MIEN1*, *MIR4642*,

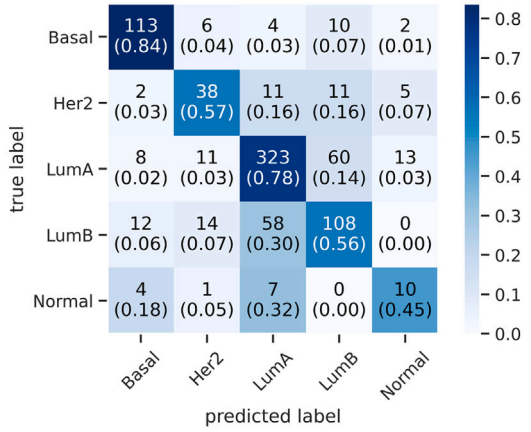

(a) Confusion Matrix signifying the number of samples correctly classified (diagonal entries) for different breast cancer subtypes using identified 44 CNV biomarkers

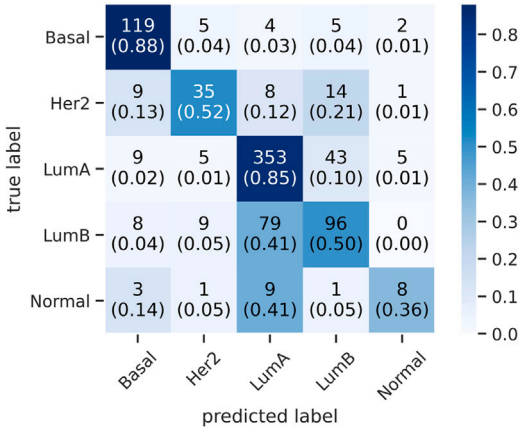

(b) Confusion Matrix signifying number of samples correctly classified (diagonal entries) for different breast cancer subtypes using PAM50 biomarkers

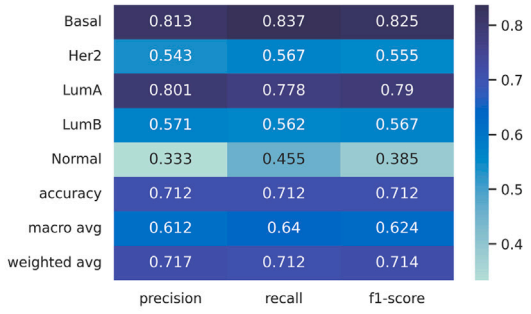

(c) Heatmap-Summarization of precision, recall, and F1-score for different breast cancer subtypes using identified 44 CNV biomarkers

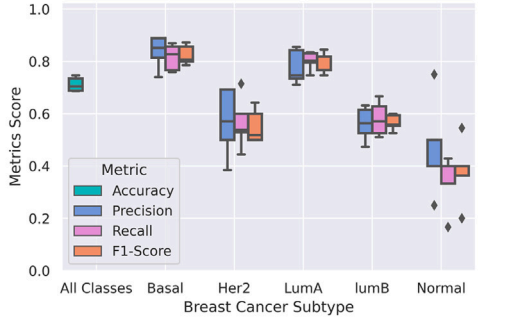

(d) BoxPlot indicating the variation in results across different breast cancer subtypes using identified 44 CNV biomarkers

Fig. 4. Classification performance of CatBoost classifier using 5 fold cross-validation for TCGA breast cancer CNV data.

MIR4728, *ORAOV1*, *OXR1*, *PGAP3*, *PNMT*, *POU5F1B*, *PPFIA1*, *PPP1R1B*, *PSMB4*, *SRGAP2B*, *STARD3*, *TCAP*, *TPCN2*, *TXNIP*, *VSTM2B*, *ZNF536*, and *snoU109*.

To estimate the efficacy of the set of 44 CNV biomarkers discovered by the proposed framework for breast cancer classification, we experimented with different classifiers. CatBoost classifier, trained using these genes achieved the best classification accuracy of 0.712 ± 0.048 at 95% confidence interval using 5-fold cross-validation. The details of the performance of the CatBoost classifier appear in Fig. 4. Diagonal entries in the confusion matrix (see Fig. 4(a)) indicate the number of samples of each class that have been correctly classified. While the model is able to predict most of the Basal (84%) and LumA (78%) samples correctly, it yields moderate performance on LumB (56%), Her2 (57%), and Normal-like breast cancer (45%) subtypes with several samples misclassified as LumA. For the Her2 subtype, the classifier is able to predict 67% of the samples correctly. The heatmap in Fig. 4(c) summarizes the classification performance in terms of precision, recall, and F1-score for five breast cancer subtypes. The model yields precision, recall, and F1-score of approx 0.80 for each of Basal and LumA. However, precision, recall, and F1-score values for Her2 and LumB were in the range [0.54, 0.57]. The model witnessed the least performance for the Normal-like subtype with precision, recall, and F1-score being 0.33, 0.45, and 0.38 respectively. However, such performance is only expected, considering a small number (22) of instances of Normal-like class. To visualize variation in performance amongst the folds during 5-fold cross-validation, box plots for accuracy, precision, recall, and F1-score the values are shown in Fig. 4(d). Note that the classifier yields the least variation for Luminal A, Luminal B, and Basal subtypes without any outlier highlighting stable results for the subtypes as compared to Luminal A and Normal-like subtype with relatively lesser samples.

We have relied upon PAM50 labels derived from transcriptomic data since PAM50 intrinsic subtypes are known for their ability to predict breast cancer survival. We also tested the PAM50 genes for their differential ability at copy number level. In this regard, we have compared the classification accuracy of the set of discovered 44 biomarker genes (see Fig. 4) obtained from CBDA and the set of PAM50 genes (see Fig. 4(b)), using the same CatBoost classifier. Although these two gene sets are derived from different genomic data, the analysis revealed the performance of the discovered set of 44 biomarkers is comparable to PAM50 genes (five-fold accuracy of 0.712 (±0.048) vs. 0.705 (±0.035) at 95% confidence interval, respectively), which again highlights the importance of CBDA derived genes.

Effect of SMOTE on CNV biomarker selection

Using SMOTE, XAI-CNVMarker yielded 44 CNV biomarkers with an accuracy of 0.712 ± 0.048. However, without using SMOTE, the framework XAI-CNVMarker yielded 67 genes and attained a reduced accuracy of 0.597 ± 0.043 at a 95% confidence interval (using 5-fold cross-validation). The confusion matrix and heatmap (Fig. 5) illustrate that most of the instances are categorized as being in the Luminal A or Luminal B class, both of which are majority classes (with almost the least number of instances classified as the Normal subtype), given the skewed class-wise distribution (Basal: 135, Her2: 67, LumA: 415, LumB: 192, and Normal-like: 22). Thus, the results of experimentation done without SMOTE show that the model got biased towards the dominant classes (Luminal A and Luminal B), which resulted in several

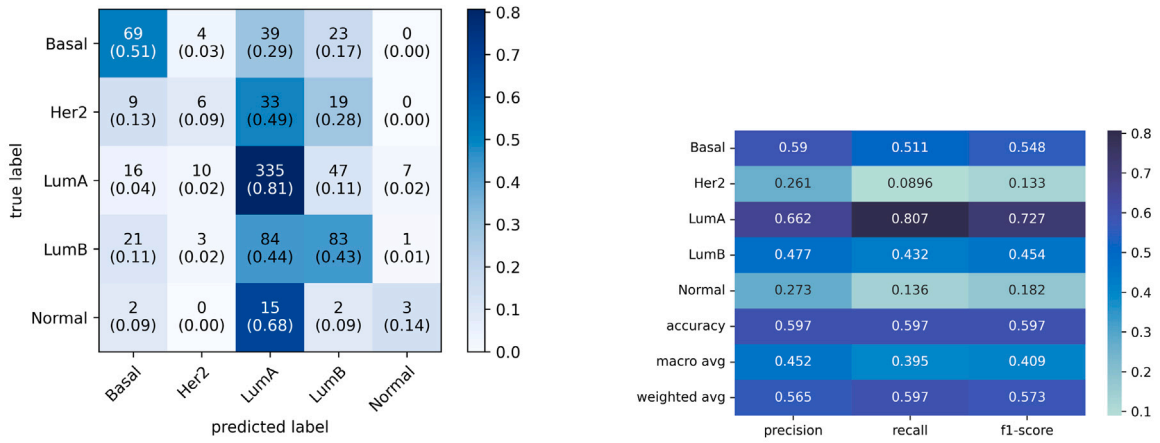

(a) Confusion Matrix signifying the number of samples correctly classified (diagonal entries) for different breast cancer subtypes using identified 67 CNV biomarkers

(b) Heatmap-Summarization of precision, recall, and F1-score for different breast cancer subtypes using identified 67 CNV biomarkers

Fig. 5. Classification performance of CatBoost classifier using 5-fold cross-validation for TCGA breast cancer without using SMOTE.

Table 1
Classification Performance for breast cancer classification on TCGA breast cancer dataset.

Method	Features	Accuracy	Macro-F1
XAI-CNVMarker	44	0.712 ± 0.048	0.624
DeepSSC [40]	248	0.705	0.606
Cristovao et al. [27]	384	0.706 ± 0.037	0.4414

CNV biomarkers being representative of the Luminal A and Luminal B classes. Not surprisingly, several instances were wrongly classified as belonging to the majority class.

Using SHAP to estimate marginal contribution of discovered 44 CNV biomarkers using SHAP

To estimate the marginal contribution of each gene in the discovered biomarker set, we applied the SHAP method to compute their SHAP values. Ranking of the genes in descending order of relevance (quantified by the average impact on model output magnitude) in the breast cancer classification task has been shown in Fig. 6. Each bar is split into five colors, namely, blue, purple, pink, brown, and green that refer to the breast cancer subtypes Luminal A, Luminal B, Basal, Her2, and Normal respectively. The width of the colors within a bar acts as a measure of the contribution (computed in terms of SHAP values) of the gene in subtype prediction. For example, *GADD45A* gene contributes most significantly towards the prediction of the subtype Luminal A, followed by Basal, Luminal B, Normal, and Her2 subtype in decreasing order of significance. Also, Figures in 7(a), 7(b), 7(c), 7(d), and 7(e) depict 15 most significant genes for Basal, Her2, Luminal A, Luminal B, and normal like subtypes respectively. In these figures, for each gene on the y-axis, the horizontal bar against it indicates the influence of copy number variation of the gene on the model's prediction. Red and blue colors indicate the amplification and deletion of copies of the genes respectively. For example, for the Basal subtype (see Fig. 7(a)), *KRT6C* is the most significant gene. Deletion of copies of *KRT6C* gene (indicated by blue color) favors the classifier in predicting the Basal class (positive impact on model's output) and amplification in its copies favors the classifier in predicting against the Basal class, i.e., breast cancer subtypes other than Basal.

3.3. Comparison with state-of-the-art frameworks

In this section, we show a comparison of our work with two state-of-the-art works: Cristovao et al. [27], Le et al. [40]. Cristovao et al. [27] used copy number alteration (CNA) data from the TCGA repository to distinguish between five PAM50 subtypes of breast cancer. Each sample comprised a probe-level vector of 1.3 million values. Pearson correlation coefficient was used to merge similar nearby regions, assigning the average copy number count to the merged region. Thus, they were able to reduce the copy number values to 384 per patient. Using logistic regression with L1 regularization, they achieved maximum accuracy of 0.706 ± 0.037. Le et al. [40] proposed a deep learning model DeepSSC for classifying TCGA BRCA patients using gene-level copy number data. They employed a denoising autoencoder for extracting compact representation followed by a feed-forward neural network for classification. They leveraged Integrated Gradients to identify a set of the top 248 genes. Although they experimented with several classifiers, they obtained the best classification accuracy of 0.705 using the random forest classifier. It is evident from Table 1 that our proposed framework- $XAI - CNVMarker$ not only yields a smaller set of 44 biomarkers but also achieves a higher accuracy of 0.712 ± 0.048.

3.4. Gene set analysis and trustworthiness of the biomarkers

In this section, we analyze the role of the set of 44 CNV biomarkers discovered by the proposed framework *XAI-CNVMarker* in breast cancer classification.

Visual analysis of CNV biomarkers

For visualizing the differential capability of the identified CNV biomarkers, we plotted heatmap and T-SNE (plotted using PROMO tool [41]). The heatmap in Fig. 8(a), shows the segregation of the instances of different breast cancer types on the basis of these biomarkers. Further, T-SNE visualization (Fig. 8(b)) shows the overall aggregated capacity of the selected CNV biomarkers in segregating Basal, LumA, and Her2 subtypes, even though Normal-like and LumB samples somewhat overlap with LumA.

Pathways enriched by CNV biomarkers

Using an over-representation test on the set of discovered 44 CNV Biomarkers, we identified 37 enriched Reactome and KEGG pathways (FDR corrected p-values less than 0.05, please see Figs. 9(a) and 9(b)). It is pertinent to note that the enriched pathways are related to breast cancer. Further, most of these pathways are enriched by eleven genes namely, *GRB7*, *ERBB2*, *ELIN2*, *FGF4*, *FGFR1*, *FGF19*, *ATAD2*, *PSMB4*, *CCND1*, *FADD*, and *GADD45A*. On closer scrutiny, we find that several pathways are closely related to different breast cancer subtypes. For example, *GRB7* events in *ERBB2* signaling pathway is known to be

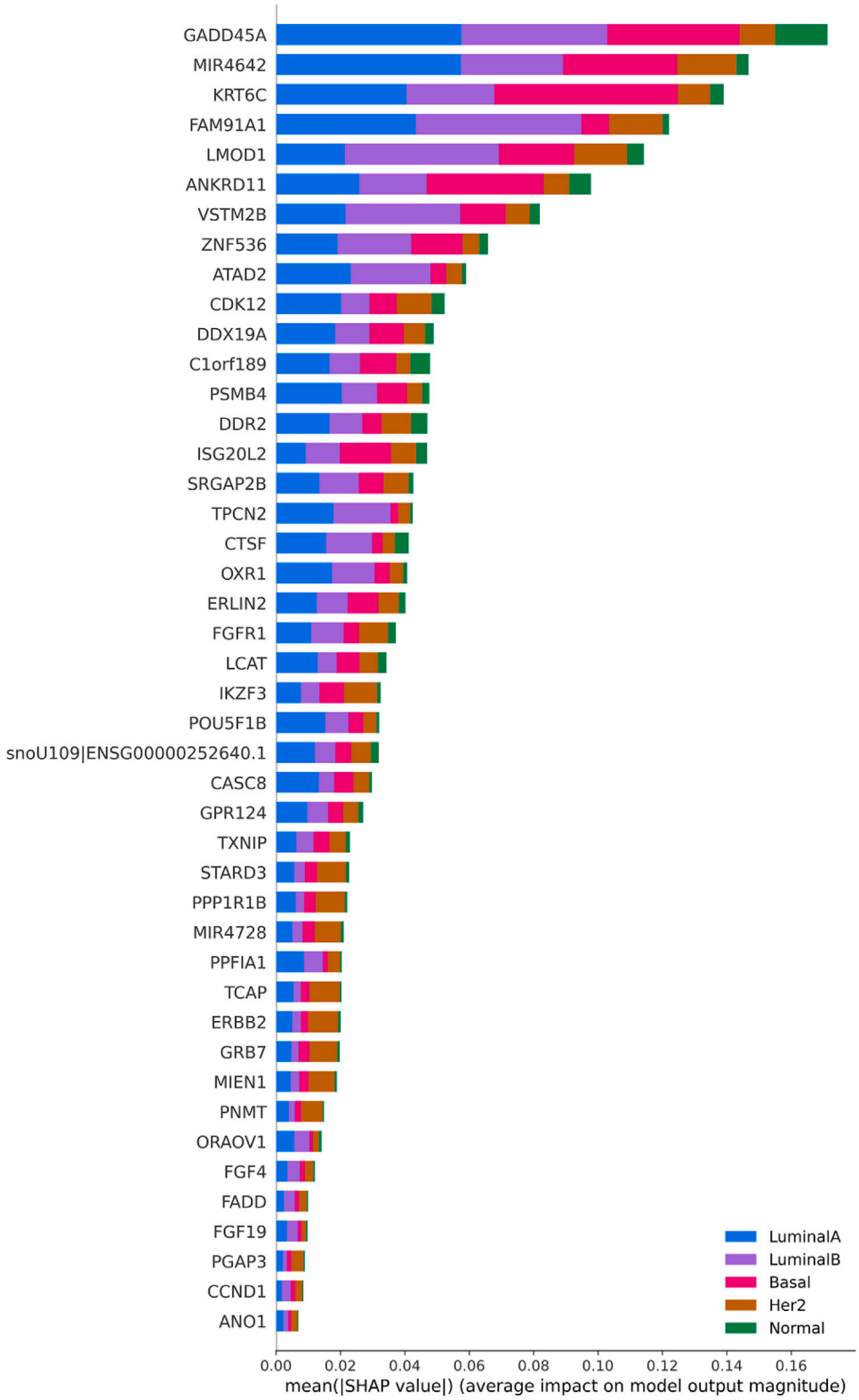

Fig. 6. Summary Plot: Genes ordered with respect to their average impact on model output.

associated with proliferation in HER2 breast tumor cells [42] caused by co-amplification of *GRB7* and *ERBB2* oncogenes. Signaling by activated point mutants of *FGFR1* pathway, enriched by *FGF4* and *FGFR1* tumor suppressor gene, is responsible for the development of Luminal A/B subtype linked with the over-representation of these genes resulting in cell proliferation and metastatic spread of this cancer subtype [43]. Similarly, *PI3K* Cascade pathway is known to be associated with oncogenic aberrations in Basal subtype [44,45]. RAF/MAP kinase cascade pathway is another pathway playing a critical role in the Basal subtype. This pathway is enriched by *ERBB2*, *FGF19*, *FGF4*, *FGFR1*, and *PSMB*

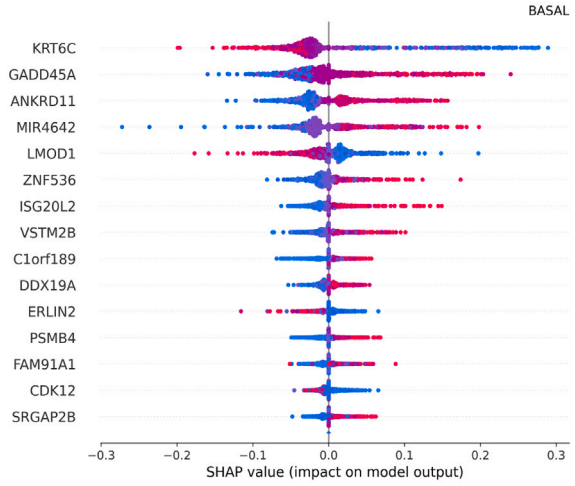

(a) Shap value of top 15 genes for Basal subtype

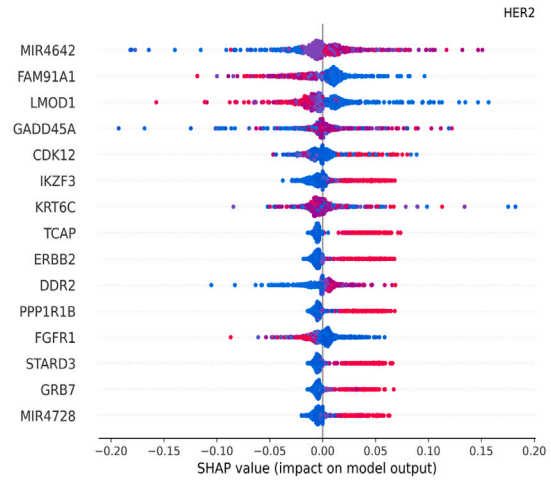

(b) Shap value of top 15 genes for Her2 subtype

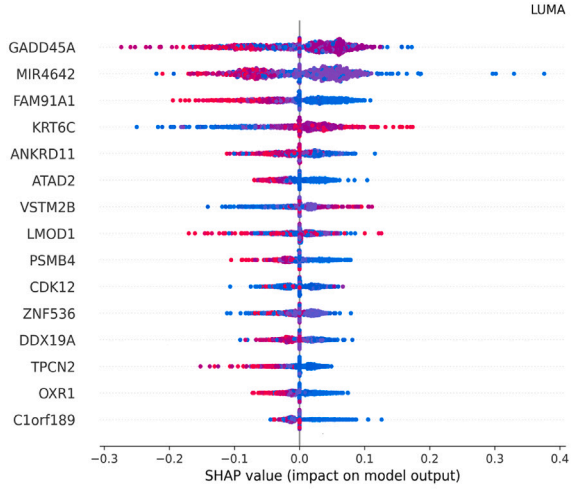

(c) Shap value of top 15 genes for Luminal A subtype

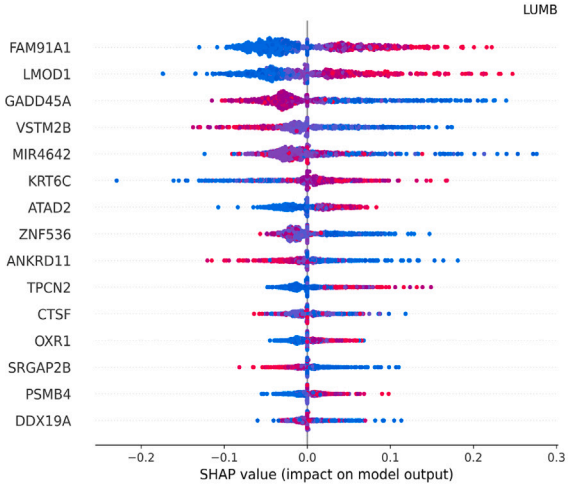

(d) Shap value of top 15 genes for Luminal B subtype

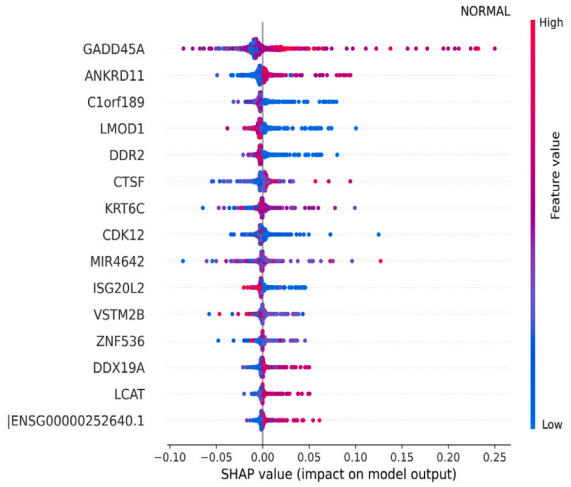

(e) Shap value of top 15 genes for Normal subtype

Fig. 7. Beeswarm Plot: Genes ordered with respect to SHAP values for each of the five breast cancer subtypes.

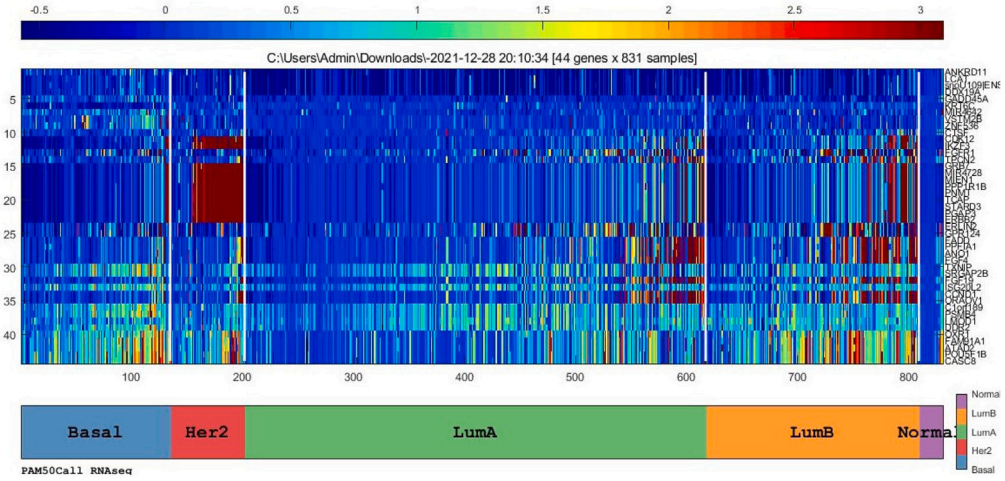

(a) Heatmap showing segregation of the instances of different breast cancer types on the basis of identified 44 CNV biomarkers

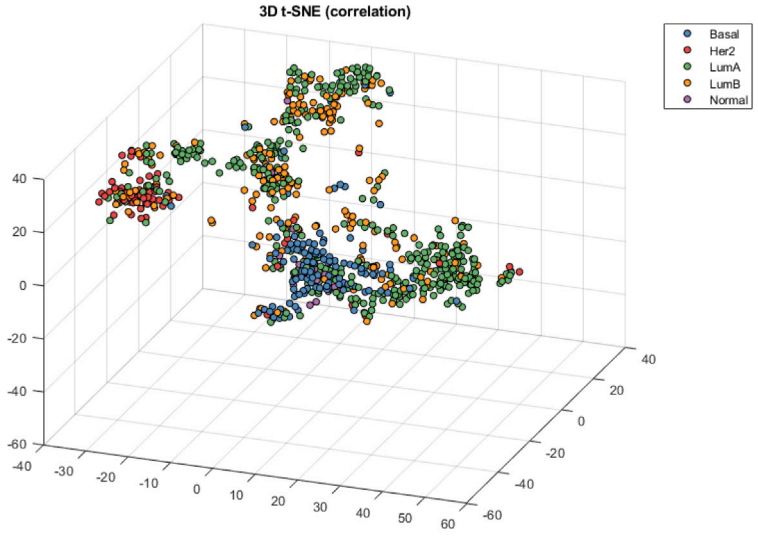

(b) T-SNE Visualization

Fig. 8. Heatmap and T-SNE Visualization using proposed 44 CNV Biomarkers.

genes and is accountable for elevation of *MEK1* and *MEK2* proteins playing the role of tumor initiation and progression [46]. For the Luminal breast cancer subtype, enriched pathway, namely, Transcriptional regulation by the AP-2 (*TFAP2*) family of transcription factors plays a significant role in its progress [47].

Druggability of CNV biomarkers

We also evaluated the discovered biomarkers for their possible use in devising treatment strategies. For this purpose, we used the Drug Gene Interaction Database (DGIdb). The CNV biomarkers discovered using the proposed framework include 21 potentially druggable genes, namely, *ANKRD11*, *ANO1*, *ATAD2*, *CCND1*, *CDK12*, *CTSF*, *DDR2*, *ERBB2*, *ERLIN2*, *FGF19*, *FGFR1*, *GADD45A*, *GPR124*, *GRB7*, *IKZF3*, *LCAT*, *PNMT*, *POU5F1B*, *PSMB4*, *TPCN2*, and *TXNIP*. For example, Ankyrin repeat domain 11 (*ANKRD11*)—a breast cancer tumor suppressor gene, is a p53-interacting protein that has the capability to enhance the transcriptional activity of p53 [48]. [49] noted that the downregulation of Ankyrin repeats domain 11 (*ANKRD11*) gene leads to the progression of Luminal A breast cancer. So, this gene may be targeted to act as a p53 co-activator. Similarly, Calcium-activated chloride channel anoctamin 1 (*ANO1*) is a gene that acts as a catalyst in breast cancer progression by activating *EGFR* and *CAMK* signaling [50]. It is located in 11q13 amplicon, a region amplified in approximately 15% of breast cancer. The study showed that if amplification of *ANO1* is suppressed, it would inhibit proliferation, aid induced apoptosis, and ultimately lead to a reduction in tumor growth.

According to a study, conducted by [51], *ATAD2* or *ANCCA* is an overexpressed gene in around 70% of breast cancers, and its high level is associated with Basal subtype. As the gene is associated with various oncogenic pathways, it may be targeted for breast cancer treatment. Also, amplification of copy number of oncogene Cyclin D1 (*CCND1*) gene encoding cyclin D1 protein in luminal B breast cancer is linked with immuno-suppression. So, drug therapy that suppresses the activity of *CCND1* gene at the protein level would prevent the progression of breast cancer (luminal B) [52,53]. Cyclin-dependent kinase (*CDK12*) acts as a tumor suppressor gene for the basal subtype, however, the gene plays the role of tumor progression for the Her2 subtype. The critical role of the gene gives direction towards using it as a potential biomarker not only for breast cancer identification but also as a therapeutic target in basal and Her2 breast carcinoma, as suggested in several studies [54,55]

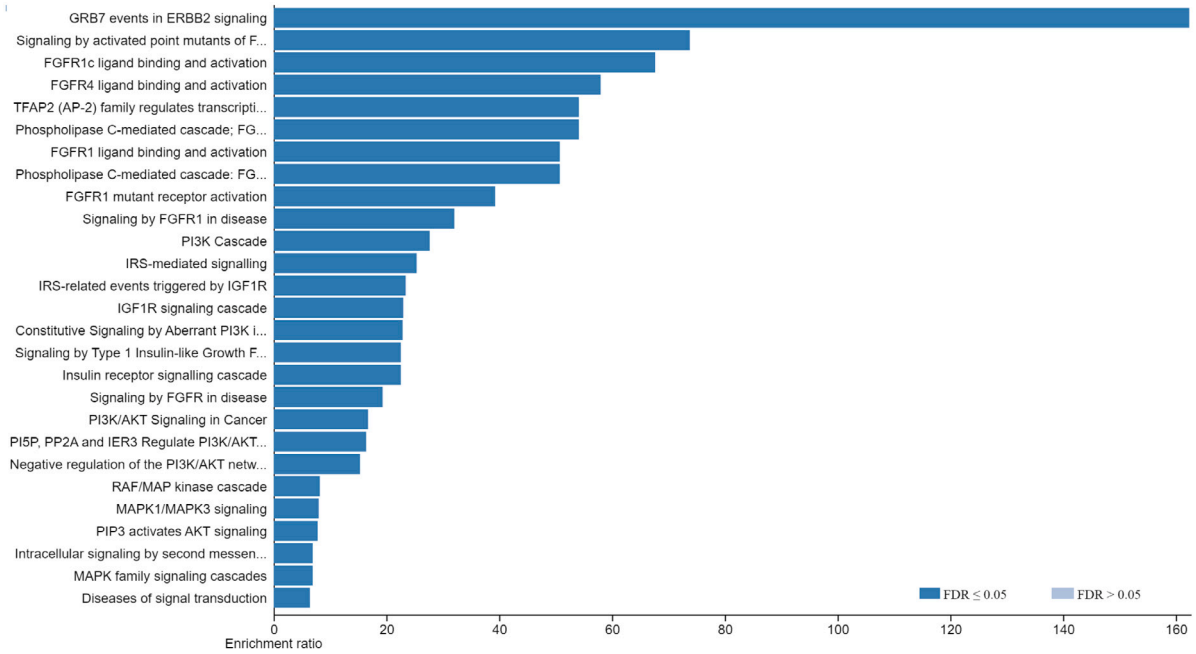

(a) Reactome Pathways Enriched by 44 proposed CNV Biomarkers

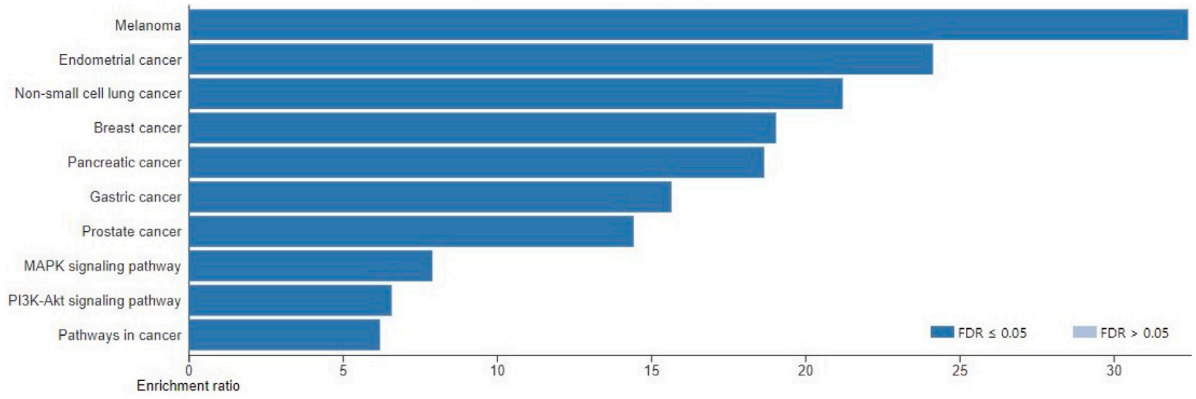

(b) KEGG Pathways Enriched by 44 proposed CNV Biomarkers

Fig. 9. Reactome and Kegg Pathways enriched using proposed 44 CNV Biomarkers.

Discoidin domain receptor 2 (DDR2), a collagen-binding receptor, has a key role in hypoxia-induced breast cancer metastasis [56]. Studies have established that inhibiting the gene can assist in preventing tumorigenesis, thus, *DDR2* may be used for targeting medication. *ERBB2* is associated with tyrosine kinase inhibitors (TKI) and variation in the number of copies of this gene is associated with variation in an individual's reaction towards the drug. Knowing the copy number variation of this gene in a patient sample can help to choose an efficient TKI drug against the tumor to enhance the chances of survival for Her2 subtype patients [57]. *GRB7*, *PNMT*, and *STARD3* genes, often co-amplified with *ERBB2* [58,59], are also associated with progression of the Her2 subtype and could be therapeutic targets for this subtype. [60] state that in breast cancer, particularly in HER2-positive patients, over-amplification of *ERBB2* is quite common. They also show that *PPP1R1B* and *IKZF3* genes are genomic neighbors of *ERBB2* gene, and they get fused with *ERBB2*, suggesting this fusion as a result of local instability. Further, the endoplasmic reticulum lipid raft-associated 2 (*ERLIN2*) gene has been found responsible for oncogenic behavior in luminal breast cancer subtype [61,62]. So, therapy that targets the downregulation of the gene will assist in reduced de novo lipogenesis, thereby preventing cancer cell proliferation.

Porta et al. [63] found Fibroblast Growth Factor Receptor (FGFR) as a promising druggable target for breast cancer. This family of genes consists of tyrosine kinase receptor (TKR) which is involved in several biological processes. Lang and Teng [64], Brady et al. [65] point out that the high activation of *FGF4* is strongly linked with amplification of other *FGF* ligands *FGF19* as well as *FGFR1*. These genes are co-amplified in Luminal B, Her2, and Basal subtypes. Thus, being oncogenes aiding in cancer development and progression, these genes could be significant therapeutic targets. Along with *FGFR1*, *GPR124* is also amplified in basal subtype patients in the chromosome region between *8p11* and *8p12* and can be targeted for devising drug therapy for the basal subtype [66–68]. *GADD45A* (growth arrest and DNA-damage-inducible protein 45 alpha) genes have been found as the downstream targets for *p53* and *BRCA1* genes which are critical in preserving genome stability and preventing tumor growth [69,70].

Similarly, recent studies suggest that *POU5F1* gene belonging to POU transcription factor family [71] and Two-pore channel 2 (*TPCN2* gene) [72] gene are also expressed in breast cancer patients and can be used as candidates for the treatment of breast cancer. Another biomarker Proteasome Subunit $\beta 4$ (*PSMB4*), a member of the ubiquitin–proteasome family, is an overexpressed gene accelerating breast cancer cell proliferation. Its use has also been suggested as a therapeutic

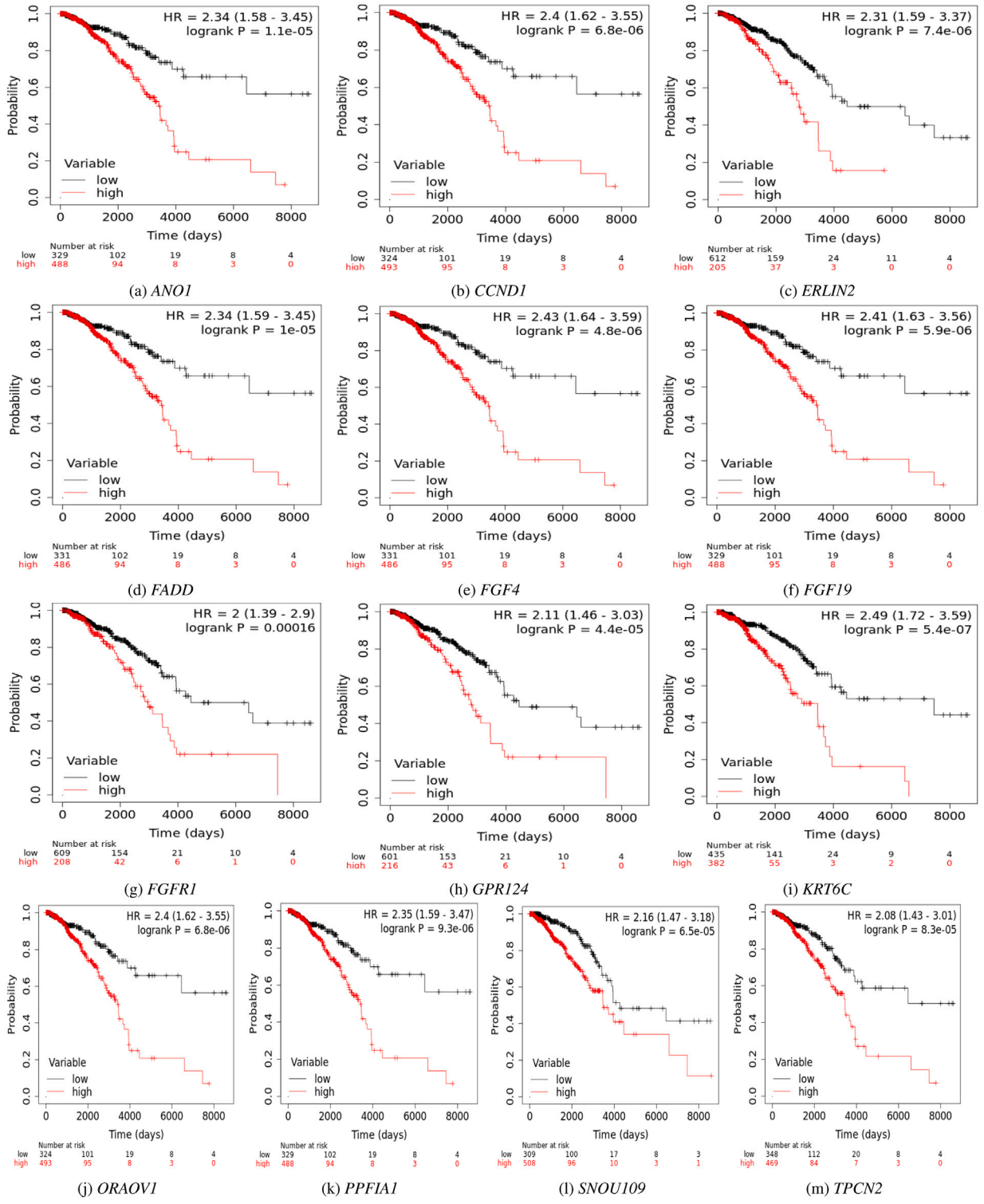

Fig. 10. Kaplan–Meier curve of top 13 survival-related genes plotted using Kaplan–Meier plotter tool.

target [73,74]. Finally, Thioredoxin-interacting protein (*TXNIP*) is a tumor suppressor gene that is downregulated in Basal patients. So, it may also be used for devising drug therapy for basal type breast cancer [75].

Prognostic analysis of CNV biomarkers

To study the role of the discovered biomarkers in prognostic evaluation, we used Kaplan–Meier (KM) plotter tool [76]. It enabled us to segregate the patients into two groups based on the CNV count. The KM plotter tool applies the best cutoff criterion to determine the split point. The tool plots Kaplan–Meier curves that depict the overall survival probabilities for each group. As 13 out of 44 genes have FDR-corrected log-rank *p*-value less than 0.05, it indicates that these genes are linked with survival. It is evident from Fig. 10 that thirteen genes, namely, *ANO1* [77], *CCND1* [78], *ERLIN2* [61], *FADD* [79], *FGFF4*, *FGF19*, *FGFR1*, *GPR124* [65,68], *KRT6C* [80], *ORAOV1* [81], *PPFIA1* [82],

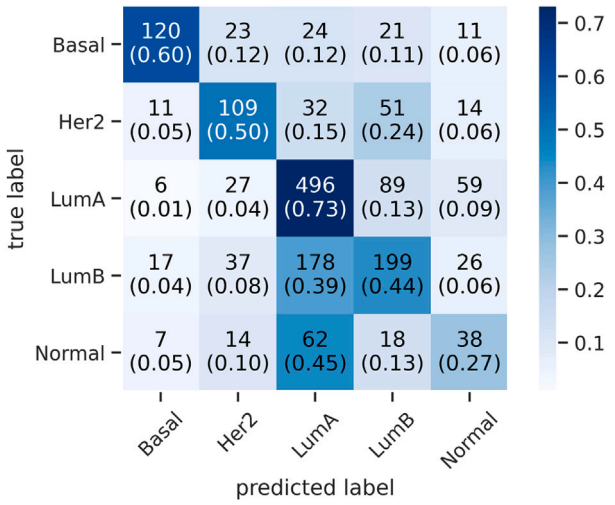

Fig. 11. Experimental results on independent cohort.

SNOU109 [83], and *TPCN2* [72] have log-rank *p*-value less than 0.05 and clearly separates the prognostic outcomes of the two groups. A hazard ratio of more than two in Kaplan–Meier curves in Figs. 10 indicates that the patients in the negative copy number variation group who are alive at any point in time, have at least twice the probability of having died as compared to patients in other positive copy number variation group.

Thus, the present algorithm has brought focus onto marker genes with prognostic and druggability potential. This could be helpful in developing clinically accepted tests for early detection and better clinical management of breast cancer patients.

3.5. Validation on independent cohort

To validate the efficacy of the proposed 44 CNV Biomarkers in breast cancer classification, we used these genes to classify the patients in the METABRIC dataset into the five breast cancer subtypes. Using the Catboost classifier, we have achieved a classification accuracy of 0.571. Fig. 11 depicts the confusion matrix for this classifier. It is evident from this figure that while the classifier achieves better accuracy for LumA and Basal subtypes, several instances of LumB and Normal-like are misclassified as LumA. This may be attributed to the fact that the Normal-like subtype-specific biomarkers have been identified using only 22 instances present in the TCGA dataset. Another group, El-Bendary et al. [84], has also experimented with the METABRIC dataset. Based on a statistical analysis of CNV data, they extracted 276 CNV features and achieved a classification accuracy of 0.534 using linear SVM and 0.549 using SVM radial. Using the same classifiers, we obtained classification accuracy of 0.537 and 0.553 respectively.

4. Conclusion

Molecular classification is an established approach for devising a subtype-specific clinical strategy. Copy number variation being more stable than other omics data leads to robust biomarkers. So, in this work, we have analyzed the variations in copy number of genes to dissect the heterogeneity of breast cancer subtypes. Towards this end, we have proposed *XAI-CNVMarker*—an explainable AI-based biomarker discovery framework. To the best of our knowledge, the proposed framework is the first attempt that exploits the power of explainable AI for discovering a small set of biomarkers, capable of differentiating amongst different breast cancer subtypes. Towards this end, we have developed *DLmodel*—a deep learning-based model for breast cancer classification which is analyzed using the proposed CNV Biomarker Discovery Algorithm (CBDA) that incorporates different explainable AI methods to mark the relative relevance of the genes. To ensure coherence amongst different interpretation methods, we consider only those genes that are marked relevant by all the explainable AI methods. Thereby, XAI-CNVMarker led to the discovery of 44 biomarkers. Subsequently, we used the Shapley Additive exPlanation (SHAP) method to rank the contribution of the selected 44 biomarkers in breast cancer classification. Using the CatBoost classifier, we obtained 5-fold cross-validation classification accuracy of 0.712 $\pm$ 0.048 at a 95% confidence interval. To establish the efficacy of the set of 44 CNV biomarkers in dissecting the heterogeneity of breast cancer, we validated their distinguishing capability on an independent cohort (METABRIC dataset).

Gene set analysis revealed 37 enriched Reactome and Kegg pathways, such as *GRB7* events in *ERBB2*, Signaling by *FGFR1* in disease, *MAPK1/MAPK2* signaling pathway, and, *PI3K-Akt* signaling pathway, known to be closely linked with different Breast Cancer subtypes. Heatmap and t-SNE visualizations demonstrate the distinguishing capability of identified biomarkers. Survival analysis using the Kaplan–Meier plots revealed that most of the discovered biomarkers (13 genes out of 44) are linked with the prognostic outcome. Also, the presence of 21 druggable genes in the set of biomarkers namely *ANKRD11*, *ANO1*, *ATAD2*, *CCND1*, *CDK12*, *CTSF*, *DDR2*, *ERBB2*, *ERLIN2*, *FGF19*, *FGFR1*, *GADD45A*, *GPR124*, *GRB7*, *IKZF3*, *LCAT*, *PNMT*, *POU5F1B*, *PSMB4*, *TPCN2*, and *TXNIP* reveals potential targets for therapeutic intervention.

In summary, the explainable AI approach has enabled us to discover a small set of 44 biomarker genes (based on copy number variation) that exhibit variations at copy number (genomic) level across different breast cancer subtypes. We have established the clinical relevance of the identified biomarkers using gene set analysis, survival analysis, and druggability analysis. The discovery of concise and clinically relevant CNV Biomarkers for breast cancer classification gives direction for the applicability of Explainable AI in biomarker discovery in oncology. In the future, we aim to provide a better understanding of mechanisms for clinicians to manage the disease efficiently. In follow-up work, we intend to incorporate multi-omic data for breast cancer classification to build upon effective and individualized clinical cancer care.

Funding

This research did not receive any grant from any of the funding agencies.

CRediT authorship contribution statement

Sheetal Rajpal: Conceived the experiments and led the development of the framework, Writing, Analysis and interpretation of the data. **Ankit Rajpal:** Writing, Analysis and interpretation of the data. **Manoj Agarwal:** Reviewed and edited the manuscript. **Virendra Kumar:** Reviewed and edited the manuscript. **Ajith Abraham:** Reviewed and edited the manuscript. **Divya Khanna:** Analysis and interpretation of the data. **Naveen Kumar:** Analysis and interpretation of the data.

Declaration of competing interest

The authors declare that they have no known competing financial interests or personal relationships that could have appeared to influence the work reported in this paper.

Data availability

Data will be made available on request.

Acknowledgments

The authors are extremely grateful to Tavpritesh Sethi, Associate Professor, IIIT Delhi for his guidance and insightful comments on the results under the PhD Clinic – ACM India Council initiative.

The fourth author would like to thank DST Women Scientist A Fellowship (WOS-A/LS-350/2017).

All authors read and approved the final draft of the manuscript.

Appendix. Background

Machine learning has been extensively used for constructing models that identify useful patterns from data and output decisions/predictions with minimum human intervention. However, the models so constructed have traditionally operated like black boxes and do not indicate the rationale behind their decisions to the end user. Fortunately, in recent years, several model-specific and model-agnostic explainable AI methods have been developed that aid in interpreting the outcome of the machine learning models. These methods attempt to answer why a model is making a given prediction and when to trust a model. Answers to such questions assist in understanding the model's behavior. One approach towards developing interpretable ML solutions could be to deploy inherently interpretable models such as a sparse decision tree or a sparse linear regression model. However, inherently interpretable models are often too simple to solve complex problems. Fortunately, there has been significant progress in recent years in the direction of making the machine learning models interpretable, resulting in the emergence of a new discipline of Explainable AI (abbreviated as X-AI or simply XAI) [85–87]. The Explainable AI methods fall into two categories, namely, model-specific and model-agnostic. Model-Specific Methods can be used for explaining the behavior of a particular type of machine learning model, while Model-agnostic Methods can be used for explaining the behavior of an arbitrary machine learning model. The following listed are four neural network-specific methods (Gradient *Input, Integrated Gradient, Epsilon Layerwise Relevance Propagation, and DeepLIFT methods) and one model-agnostic method, namely, SHAP.

- Gradient*Input: The gradient method [88] employs backward propagation on the trained network to identify which input features will trigger the weights and activation of the output layer. Given a prediction of the neural network model at the output layer, the gradient method backpropagates the gradients at each layer to quantify the contribution (also called attribution or relevance score) of each input feature in the prediction. The attributions produced by the gradient method are collectively known as the saliency maps. In other words, the saliency maps highlight the most important features which assist the proposed network in predicting a class. For a given layer l, the partial derivative of its output with respect to the previous layer is computed using the following equation:

$$\frac{\delta A^l}{\delta A^{l-1}} \tag{1}$$

  Back propagating the partial derivatives in this manner, $\frac{\delta A^l}{\delta X}$ (partial derivative with respect to input X) yields the gradients or the saliency map. Gradient*input is a variant of the basic gradient method that computes the feature attributions by multiplying the gradient by the input feature. Thus, it is able to avoid the problem of saturating gradients.
- Integrated Gradient: Integrated gradient method [89] deals with the problem of noisy gradients by computing the integral of gradients of several instances generated through linear interpolation between the baseline input (X') and original input (X). For example, for images, considering the baseline image to be an image with all pixels set to black, interpolated images are generated between this baseline and input image in small steps of α that steadily rise with the intensity of each interpolated image. Thereafter, for the ith feature in consideration, the integrated gradient may be computed using the following Eq. (2):

$$IntGrad_i(X) = (X_i - X_i') \int_{\alpha=0}^{1} \frac{\delta(F(X' + \alpha(X - X_i')))}{\delta(X_i)} \delta\alpha \tag{2}$$

- Layerwise Relevance Propagation: During the forward propagation, the activations in each layer are computed using the inputs from the previous layer. The Layerwise Relevance Propagation (LRP) method [90] back propagates the relevance (activation) of the output layer neurons by redistributing the output (relevance) to neurons in the previous layers, layer by layer, up to the input layer. The contribution a neuron i (R_i) at a layer to neuron j (R_j) in the previous layer is computed as follows:

$$R_j = \sum_i (\alpha \frac{a_j w_{ji}^+}{\sum_j (a_j w_{ji}^+)} - \gamma \frac{a_j w_{ji}^-}{\sum_j (a_j w_{ji}^-)} R_i) \tag{3}$$

  Here α and γ denote the weight that may be assigned to positive and negative influences marked by neurons with positive and negative weights i.e. w_{ji}^+ and w_{ji}^- respectively with activation of neurons denoted by a_j. In another variant of simple LRP, termed epsilon LRP, a small positive term ϵ is added to the denominator in the above expression to compensate for a weak or conflicting contribution.
- DeepLIFT: DeepLIFT (Deep Learning Important FeaTures) method [91] deconstructs the output of a neural network for a specific input, by back-propagating the relevance scores of all neurons from the output layer to the input layer. For achieving this, DeepLIFT evaluates the activation of each neuron and compares it with the "reference activation" to finally compute the relevance scores based on the difference. As compared to other methods, DeepLIFT can uncover dependencies that other techniques overlook by taking into account positive and negative contributions separately. The relevance scores are effectively computed in a single backward pass.
- SHAP: Lundberg and Lee proposed the Shapley Additive exPlanation (SHAP) method [92]—a model-agnostic tool for explaining predictions of machine learning models. It operates by quantifying the overall contribution (marginal contribution quantified by SHAPley/SHAP values) of different features in a post-hoc manner. It can be used to describe the summarized behavior of a model in terms of the input features as well as explain the contribution of different features in making predictions for a specific instance.

References

[1] H. Sung, J. Ferlay, R.L. Siegel, M. Laversanne, I. Soerjomataram, A. Jemal, F. Bray, Global cancer statistics 2020: GLOBOCAN estimates of incidence and mortality worldwide for 36 cancers in 185 countries, CA: Cancer J. Clin. 71 (3) (2021) 209–249.

[2] C.S. Vallejos, H.L. Gómez, W.R. Cruz, J.A. Pinto, R.R. Dyer, R. Velarde, et al., Breast cancer classification according to immunohistochemistry markers: subtypes and association with clinicopathologic variables in a peruvian hospital database, Clin. Breast Cancer 10 (4) (2010) 294–300.

[3] M.C. Cheang, S.K. Chia, D. Voduc, D. Gao, S. Leung, J. Snider, et al., Ki67 index, HER2 status, and prognosis of patients with luminal B breast cancer, JNCI: J. Natl. Cancer Inst. 101 (10) (2009) 736–750.

[4] C.M. Perou, T. Sørlie, M.B. Eisen, M. Van De Rijn, S.S. Jeffrey, C.A. Rees, et al., Molecular portraits of human breast tumours, Nature 406 (6797) (2000) 747–752.

[5] T. Sørlie, R. Tibshirani, J. Parker, T. Hastie, J.S. Marron, A. Nobel, et al., Repeated observation of breast tumor subtypes in independent gene expression data sets, Proc. Natl. Acad. Sci. 100 (14) (2003) 8418–8423.

[6] S. Chakraborty, M. Hosen, M. Ahmed, H.U. Shekhar, et al., Onco-multi-OMICS approach: A new frontier in cancer research, BioMed Res. Int. 2018 (2018).

[7] X. Liu, Y. Peng, J. Wang, Integrative analysis of DNA methylation and gene expression profiles identified potential breast cancer-specific diagnostic markers, Biosci. Rep. 40 (5) (2020) BSR20201053.

[8] S. Rakshit, I. Saha, S.S. Chakraborty, D. Plewczyski, Deep learning for integrated analysis of breast cancer subtype specific multi-omics data, in: TENCON 2018-2018 IEEE Region 10 Conference, IEEE, 2018, pp. 1917–1922.

[9] J. Xu, P. Wu, Y. Chen, Q. Meng, H. Dawood, H. Dawood, A hierarchical integration deep flexible neural forest framework for cancer subtype classification by integrating multi-omics data, BMC Bioinformatics 20 (1) (2019) 1–11.

[10] Y. Lin, W. Zhang, H. Cao, G. Li, W. Du, Classifying Breast Cancer Subtypes Using Deep Neural Networks Based on Multi-Omics Data, Genes 11 (8) (2020) 888.

[11] C. Peng, Y. Zheng, D.-S. Huang, Capsule network based modeling of multi-omics data for discovery of breast cancer-related genes, IEEE/ACM Trans. Comput. Biol. Bioinform. 17 (5) (2019) 1605–1612.

[12] S. Pirmoradi, M. Teshnehlab, N. Zarghami, A. Sharifi, A self-organizing deep neuro-fuzzy system approach for classification of kidney cancer subtypes using miRNA genomics data, Comput. Methods Programs Biomed. 206 (2021) 106132.

[13] J.S. Parker, M. Mullins, M.C. Cheang, S. Leung, D. Voduc, T. Vickery, et al., Supervised risk predictor of breast cancer based on intrinsic subtypes, J. Clin. Oncol. 27 (8) (2009) 1160.

[14] H.K. Kim, K.H. Park, Y. Kim, S.E. Park, H.S. Lee, S.W. Lim, et al., Discordance of the PAM50 intrinsic subtypes compared with immunohistochemistry-based surrogate in breast cancer patients: Potential implication of genomic alterations of discordance, Cancer Res. Treat.: Off. J. Korean Cancer Assoc. 51 (2) (2019) 737–747.

[15] S.A. Eccles, E.O. Aboagye, S. Ali, A.S. Anderson, J. Armes, F. Berditchevski, et al., Critical research gaps and translational priorities for the successful prevention and treatment of breast cancer, Breast Cancer Res. 15 (5) (2013) 1–37.

[16] M. List, A.-C. Hauschild, Q. Tan, T.A. Kruse, J. Baumbach, R. Batra, Classification of breast cancer subtypes by combining gene expression and DNA methylation data, J. Integr. Bioinform. 11 (2) (2014) 1–14.

[17] L. Chen, T. Zeng, X. Pan, Y.-H. Zhang, T. Huang, Y.-D. Cai, Identifying methylation pattern and genes associated with breast cancer subtypes, Int. J. Mol. Sci. 20 (17) (2019) 4269.

[18] S. Zhang, J. Wang, T. Ghoshal, D. Wilkins, Y.-Y. Mo, Y. Chen, Y. Zhou, lncRNA gene signatures for prediction of breast cancer intrinsic subtypes and prognosis, Genes 9 (2) (2018) 65.

[19] B.-Q. Li, J. You, T. Huang, Y.-D. Cai, Classification of non-small cell lung cancer based on copy number alterations, PLoS One 9 (2) (2014) e88300.

[20] A. Bergamaschi, Y.H. Kim, P. Wang, T. Sørlie, T. Hernandez-Boussard, P.E. Lonning, et al., Distinct patterns of DNA copy number alteration are associated with different clinicopathological features and gene-expression subtypes of breast cancer, Genes Chromosom. Cancer 45 (11) (2006) 1033–1040.

[21] X. Pan, X. Hu, Y.-H. Zhang, L. Chen, L. Zhu, S. Wan, T. Huang, Y.-D. Cai, Identification of the copy number variant biomarkers for breast cancer subtypes, Mol. Genetics Genomics 294 (1) (2019) 95–110.

[22] C. Gao, J. Zhuang, H. Li, C. Liu, C. Zhou, L. Liu, et al., Development of a risk scoring system for evaluating the prognosis of patients with Her2-positive breast cancer, Cancer Cell Int. 20 (2020) 1–12.

[23] T.I. Zack, S.E. Schumacher, S.L. Carter, A.D. Cherniack, G. Saksena, B. Tabak, et al., Pan-cancer patterns of somatic copy number alteration, Nature Genet. 45 (10) (2013) 1134–1140.

[24] G. Wang, D. Anastassiou, Pan-cancer driver copy number alterations identified by joint expression/CNA data analysis, Sci. Rep. 10 (1) (2020) 1–10.

[25] H.R. Ali, O.M. Rueda, S.-F. Chin, C. Curtis, M.J. Dunning, S.A. Aparicio, C. Caldas, Genome-driven integrated classification of breast cancer validated in over 7,500 samples, Genome Biol. 15 (8) (2014) 1–14.

[26] C. Curtis, S.P. Shah, S.-F. Chin, G. Turashvili, O.M. Rueda, M.J. Dunning, et al., The genomic and transcriptomic architecture of 2,000 breast tumours reveals novel subgroups, Nature 486 (7403) (2012) 346–352.

[27] F. Cristovao, S. Cascianelli, A. Canakoglu, M. Carman, L. Nanni, P. Pinoli, M. Masseroli, Investigating deep learning based breast cancer subtyping using pan-cancer and multi-omic data, IEEE/ACM Trans. Comput. Biol. Bioinform. (2020).

[28] M. Tao, T. Song, W. Du, S. Han, C. Zuo, Y. Li, Y. Wang, Z. Yang, Classifying breast cancer subtypes using multiple kernel learning based on omics data, Genes 10 (3) (2019) 200.

[29] M. Sardana, R. Agrawal, B. Kaur, A hybrid of clustering and quantum genetic algorithm for relevant genes selection for cancer microarray data, Int. J. Knowl.-Based Intell. Eng. Syst. 20 (3) (2016) 161–173.

[30] L. Zhang, J. Tan, D. Han, H. Zhu, From machine learning to deep learning: Progress in machine intelligence for rational drug discovery, Drug Discov. Today 22 (11) (2017) 1680–1685.

[31] F.A. Spanhol, L.S. Oliveira, C. Petitjean, L. Heutte, Breast cancer histopathological image classification using convolutional neural networks, in: 2016 International Joint Conference on Neural Networks, IJCNN, IEEE, 2016, pp. 2560–2567.

[32] Y. Xu, Z. Jia, L.-B. Wang, Y. Ai, F. Zhang, M. Lai, et al., Large scale tissue histopathology image classification, segmentation, and visualization via deep convolutional activation features, BMC Bioinformatics 18 (1) (2017) 281.

[33] E.M. Karabulut, T. Ibrikci, Discriminative deep belief networks for microarray based cancer classification, Biomed. Res.-Tokyo 28 (3) (2017) 1016–1024.

[34] R. Fakoor, F. Ladhak, A. Nazi, M. Huber, Using deep learning to enhance cancer diagnosis and classification, in: Proceedings of the International Conference on Machine Learning, Vol. 28, ACM, New York, USA, 2013.

[35] R. Singh, J. Lanchantin, G. Robins, Y. Qi, DeepChrome: Deep-learning for predicting gene expression from histone modifications, Bioinformatics 32 (17) (2016) i639–i648.

[36] TCGA, UCSC Xena, 2022, https://xenabrowser.net/datapages/?dataset=TCGA.BRCA.sampleMap%2FGistic2_CopyNumber_Gistic2_all_data_by_genes&host=https%3A%2F%2Ftcga.xenahubs.net&removeHub=https%3A%2F%2Fxena.treehouse.gi.ucsc.edu%3A443. (Accessed on 06 June 2022).

[37] E. Cerami, J. Gao, U. Dogrusoz, B.E. Gross, S.O. Sumer, B.A. Aksoy, et al., The cBio Cancer Genomics Portal: An Open Platform for Exploring Multidimensional Cancer Genomics Data, AACR, 2012.

[38] J. Gao, B.A. Aksoy, U. Dogrusoz, G. Dresdner, B. Gross, S.O. Sumer, et al., Integrative analysis of complex cancer genomics and clinical profiles using the cBioPortal, Sci. Signal. 6 (269) (2013) pl1.

[39] N.V. Chawla, K.W. Bowyer, L.O. Hall, W.P. Kegelmeyer, SMOTE: Synthetic minority over-sampling technique, J. Artificial Intelligence Res. 16 (2002) 321–357.

[40] H. Le, V.-M. Nguyen, Q.-H. Nguyen, D.-H. Le, A biphasic deep semi-supervised framework for suptype classification and biomarker discovery, 2022, BioRxiv, Cold Spring Harbor Laboratory.

[41] D. Netanely, N. Stern, I. Laufer, R. Shamir, PROMO: An interactive tool for analyzing clinically-labeled multi-omic cancer datasets, BMC Bioinformatics 20 (1) (2019) 1–10.

[42] M.A. Olayioye, Intracellular signaling pathways of ErbB2/HER-2 and family members, Breast Cancer Res. 3 (6) (2001) 1–5.

[43] M.F. Santolla, M. Maggiolini, The FGF/FGFR system in breast cancer: Oncogenic features and therapeutic perspectives, Cancers 12 (10) (2020) 3029.

[44] D. Miricescu, A. Totan, I.-I. Stanescu-Spinu, S.C. Badoiu, C. Stefani, et al., PI3K/AKT/mTOR signaling pathway in breast cancer: From molecular landscape to clinical aspects, Int. J. Mol. Sci. 22 (1) (2021) 173.

[45] J. Pascual, N. Turner, Targeting the PI3-kinase pathway in triple-negative breast cancer, Ann. Oncol. 30 (7) (2019) 1051–1060.

[46] P.J. Roberts, C.J. Der, Targeting the Raf-MEK-ERK mitogen-activated protein kinase cascade for the treatment of cancer, Oncogene 26 (22) (2007) 3291–3310.

[47] M. Orlic-Milacic, TFAP2 (AP-2) family regulates transcription of growth factors and their receptors, 2016, URL https://reactome.org/content/detail/R-HSA-8866910.

[48] P.M. Neilsen, K.M. Cheney, C.-W. Li, J.D. Chen, J.E. Cawrse, R.B. Schulz, et al., Identification of ANKRD11 as a p53 coactivator, J. Cell Sci. 121 (21) (2008) 3541–3552.

[49] S.P. Lim, N.C. Wong, R.J. Suetani, K. Ho, J.L. Ng, P.M. Neilsen, P.G. Gill, R. Kumar, D.F. Callen, Specific-site methylation of tumour suppressor ANKRD11 in breast cancer, Eur. J. Cancer 48 (17) (2012) 3300–3309.

[50] A. Britschgi, A. Bill, H. Brinkhaus, C. Rothwell, I. Clay, S. Duss, et al., Calcium-activated chloride channel ANO1 promotes breast cancer progression by activating EGFR and CAMK signaling, Proc. Natl. Acad. Sci. 110 (11) (2013) E1026–E1034, http://dx.doi.org/10.1073/pnas.1217072110.

[51] E.V. Kalashnikova, A.S. Revenko, A.T. Gemo, N.P. Andrews, C.G. Tepper, J.X. Zou, et al., ANCCA/ATAD2 Overexpression Identifies Breast Cancer Patients with Poor Prognosis, Acting to Drive Proliferation and Survival of Triple-Negative Cells through Control of B-Myb and EZH2, Cancer Res. 70 (22) (2010) 9402–9412, http://dx.doi.org/10.1158/0008-5472.CAN-10-1199, arXiv:https://cancerres.aacrjournals.org/content/70/22/9402.full.pdf, URL https://cancerres.aacrjournals.org/content/70/22/9402.

[52] J.S. Reis-Filho, K. Savage, M.B.K. Lambros, M. James, D. Steele, R.L. Jones, M. Dowsett, Cyclin D1 protein overexpression and CCND1 amplification in breast carcinomas: an immunohistochemical and chromogenic in situ hybridisation analysis, Modern Pathol. 19 (7) (2006) 999–1009, http://dx.doi.org/10.1038/modpathol.3800621.

[53] Y. Chen, Y. Huang, X. Gao, Y. Li, J. Lin, L. Chen, et al., CCND1 Amplification contributes to immunosuppression and is associated with a poor prognosis to immune checkpoint inhibitors in solid tumors, Front. Immunol. 11 (2020) 1620.

[54] V. Quereda, S. Bayle, F. Vena, S.M. Frydman, A. Monastyrskyi, W.R. Roush, D.R. Duckett, Therapeutic Targeting of CDK12/CDK13 in Triple-Negative Breast Cancer, Cancer Cell 36 (5) (2019) 545–558.e7, http://dx.doi.org/10.1016/j.ccell.2019.09.004.

[55] S. Liang, L. Hu, Z. Wu, Z. Chen, S. Liu, X. Xu, A. Qian, CDK12: A potent target and biomarker for human cancer therapy, Cells 9 (6) (2020) 1483.

[56] T. Ren, W. Zhang, X. Liu, H. Zhao, J. Zhang, J. Zhang, et al., Discoidin domain receptor 2 (DDR2) promotes breast cancer cell metastasis and the mechanism implicates epithelial–mesenchymal transition programme under hypoxia, J. Pathol. 234 (4) (2014) 526–537.

[57] C.L. Arteaga, J.A. Engelman, ERBB receptors: From oncogene discovery to basic science to mechanism-based cancer therapeutics, Cancer Cell 25 (3) (2014) 282–303, http://dx.doi.org/10.1016/j.ccr.2014.02.025.

[58] K.K. Sahlberg, V. Hongisto, H. Edgren, R. Mäkelä, K. Hellström, E.U. Due, et al., The HER2 amplicon includes several genes required for the growth and survival of HER2 positive breast cancer cells, Mol. Oncol. 7 (3) (2012) 392–401, http://dx.doi.org/10.1016/j.molonc.2012.10.012.

[59] B. Ramsey, T. Bai, A.H. Newell, M. Troxell, B. Park, S. Olson, E. Keenan, S.-W. Luoh, GRB7 protein over-expression and clinical outcome in breast cancer, Breast Cancer Res. Treat. 127 (3) (2010) 659–669, http://dx.doi.org/10.1007/s10549-010-1010-0.

[60] Q. Gao, W.-W. Liang, S.M. Foltz, G. Mutharasu, R.G. Jayasinghe, S. Cao, et al., Driver Fusions and Their Implications in the Development and Treatment of Human Cancers, Cell Rep. 23 (1) (2018) 227–238.e3, http://dx.doi.org/10.1016/j.celrep.2018.03.050.

[61] G. Wang, G. Liu, X. Wang, S. Sethi, R. Ali-Fehmi, J. Abrams, Z. Zheng, K. Zhang, S. Ethier, Z.-Q. Yang, ERLIN2 promotes breast cancer cell survival by modulating endoplasmic reticulum stress pathways, BMC Cancer 12 (1) (2012) 1–11.

[62] G. Wang, X. Zhang, J.-S. Lee, X. Wang, Z.-Q. Yang, K. Zhang, Endoplasmic reticulum factor ERLIN2 regulates cytosolic lipid content in cancer cells, Biochem. J. 446 (3) (2012) 415–425.

[63] R. Porta, R. Borea, A. Coelho, S. Khan, A. Araújo, P. Reclusa, et al., FGFR a promising druggable target in cancer: Molecular biology and new drugs, Crit. Rev. Oncol./Hematology 113 (2017) 256–267, http://dx.doi.org/10.1016/j.critrevonc.2017.02.018.

[64] L. Lang, Y. Teng, Fibroblast Growth Factor Receptor 4 Targeting in Cancer: New Insights into Mechanisms and Therapeutic Strategies, Cells 8 (1) (2019) 31, http://dx.doi.org/10.3390/cells8010031.

[65] N.J. Brady, P. Chuntova, L.K. Bade, K.L. Schwertfeger, The FGF/FGF receptor axis as a therapeutic target in breast cancer, Exp. Rev. Endocrinol. Metabol. 8 (4) (2013) 391–402.

[66] F. Andre, B. Job, P. Dessen, A. Tordai, S. Michiels, C. Liedtke, et al., Molecular characterization of breast cancer with high-resolution oligonucleotide comparative genomic hybridization array, Clin. Cancer Res. 15 (2) (2009) 441–451.

[67] D.G. Holland, A. Burleigh, A. Git, M.A. Goldgraben, P.A. Perez-Mancera, S.-F. Chin, et al., ZNF703 is a common Luminal B breast cancer oncogene that differentially regulates luminal and basal progenitors in human mammary epithelium, EMBO Mol. Med. 3 (3) (2011) 167–180.

[68] G.N. Hortobagyi, D. Chen, M. Piccart, H.S. Rugo, H.A. Burris III, K.I. Pritchard, et al., Correlative analysis of genetic alterations and everolimus benefit in hormone receptor–positive, human epidermal growth factor receptor 2–negative advanced breast cancer: Results from BOLERO-2, J. Clin. Oncol. 34 (5) (2016) 419.

[69] J. Wang, Y. Wang, F. Long, F. Yan, N. Wang, Y. Wang, The expression and clinical significance of GADD45A in breast cancer patients, PeerJ 6 (2018) e5344.

[70] S. Pietrasik, G. Zajac, J. Morawiec, M. Soszynski, M. Fila, J. Blasiak, Interplay between BRCA1 and GADD45A and its potential for nucleotide excision repair in breast cancer pathogenesis, Int. J. Mol. Sci. 21 (3) (2020) 870.

[71] F.-Q. Zhao, Y. Misra, D.-B. Li, M.P. Wadsworth, D. Krag, D. Weaver, et al., Differential expression of Oct3/4 in human breast cancer and normal tissues, Int. J. Oncol. 52 (6) (2018) 2069–2078.

[72] A.F. Alharbi, J. Parrington, Endolysosomal Ca2+ signaling in cancer: The role of TPC2, from tumorigenesis to metastasis, Front. Cell Dev. Biol. 7 (2019) 302.

[73] H. Wang, Z. He, L. Xia, W. Zhang, L. Xu, X. Yue, X. Ru, Y. Xu, PSMB4 overexpression enhances the cell growth and viability of breast cancer cells leading to a poor prognosis, Oncol. Rep. (2018).

[74] H. Wang, Z. He, L. Xia, W. Zhang, L. Xu, X. Yue, et al., PSMB4 overexpression enhances the cell growth and viability of breast cancer cells leading to a poor prognosis, Oncol. Rep. 40 (4) (2018) 2343–2352.

[75] Y. Chen, J. Ning, W. Cao, S. Wang, T. Du, J. Jiang, et al., Research progress of TXNIP as a tumor suppressor gene participating in the metabolic reprogramming and oxidative stress of cancer cells in various cancers, Front. Oncol. 10 (2020).

[76] Á. Nagy, A. Lánczky, O. Menyhárt, B. Győrffy, Validation of miRNA prognostic power in hepatocellular carcinoma using expression data of independent datasets, Sci. Rep. 8 (1) (2018) 1–9.

[77] H. Wu, S. Guan, M. Sun, Z. Yu, L. Zhao, M. He, et al., Ano1/TMEM16A overexpression is associated with good prognosis in PR-positive or HER2-negative breast cancer patients following tamoxifen treatment, PLoS One 10 (5) (2015) e0126128.

[78] A. Lundberg, L.S. Lindström, J. Li, J.C. Harrell, E. Darai-Ramqvist, E.G. Sifakis, et al., The long-term prognostic and predictive capacity of cyclin D1 gene amplification in 2305 breast tumours, Breast Cancer Res. 21 (1) (2019) 1–10.

[79] E.J. Choi, J.A. Yun, S. Jabeen, E.K. Jeon, H.S. Won, Y.H. Ko, S.Y. Kim, Prognostic significance of TMEM16A, PPFIA1, and FADD expression in invasive ductal carcinoma of the breast, World J. Surg. Oncol. 12 (1) (2014) 1–7.

[80] W.-H. Kuo, Y.-Y. Chang, L.-C. Lai, M.-H. Tsai, C.K. Hsiao, K.-J. Chang, E.Y. Chuang, Molecular characteristics and metastasis predictor genes of triple-negative breast cancer: A clinical study of triple-negative breast carcinomas, PLoS One 7 (9) (2012).

[81] X. Yue, L. Zhou, W. Wong, et al., ORAOV1 and WWOX are metastatic and prognostic biomarker for invasive breast cancer, Int. J. Clin. Exp. Med. 10 (2017) 13607–13615.

[82] J. Yang, N.-N. Wu, D.-J. Huang, Y.-C. Luo, J.-Z. Huang, H.-Y. He, et al., PPFIA1 is upregulated in liver metastasis of breast cancer and is a potential poor prognostic indicator of metastatic relapse, Tumor Biol. 39 (7) (2017) 1010428317713492.

[83] V.L. Dsouza, D. Adiga, S. Sriharikrishnaa, P.S. Suresh, A. Chatterjee, S.P. Kabekkodu, Small nucleolar RNA and its potential role in breast cancer–A comprehensive review, Biochim. Biophys. Acta (BBA)-Rev. Cancer (2021) 188501.

[84] N. El-Bendary, N.A. Belal, et al., A feature-fusion framework of clinical, genomics, and histopathological data for METABRIC breast cancer subtype classification, Appl. Soft Comput. 91 (2020) 106238.

[85] A. Holzinger, C. Biemann, C.S. Pattichis, D.B. Kell, What do we need to build explainable AI systems for the medical domain? 2017, arXiv preprint arXiv:1712.09923.

[86] A.B. Arrieta, N. Díaz-Rodríguez, J. Del Ser, A. Bennetot, S. Tabik, A. Barbado, et al., Explainable Artificial Intelligence (XAI): Concepts, taxonomies, opportunities and challenges toward responsible AI, Inf. Fusion 58 (2020) 82–115.

[87] D. Doran, S. Schulz, T.R. Besold, What does explainable AI really mean? A new conceptualization of perspectives, 2017, arXiv preprint arXiv:1710.00794.

[88] K. Simonyan, A. Vedaldi, A. Zisserman, Deep inside convolutional networks: Visualising image classification models and saliency maps, 2013, arXiv preprint arXiv:1312.6034.

[89] M. Sundararajan, A. Taly, Q. Yan, Axiomatic attribution for deep networks, in: International Conference on Machine Learning, PMLR, 2017, pp. 3319–3328.

[90] S. Bach, A. Binder, G. Montavon, F. Klauschen, K.-R. Müller, W. Samek, On pixel-wise explanations for non-linear classifier decisions by layer-wise relevance propagation, PLoS One 10 (7) (2015) e0130140.

[91] A. Shrikumar, P. Greenside, A. Kundaje, Learning important features through propagating activation differences, in: International Conference on Machine Learning, PMLR, 2017, pp. 3145–3153.

[92] S.M. Lundberg, S.-I. Lee, A unified approach to interpreting model predictions, in: Proceedings of the 31st International Conference on Neural Information Processing Systems, 2017, pp. 4768–4777.